Available online at www.ijournalse.org

Emerging Science Journal

(ISSN: 2610-9182)

Vol. 10, No. 1, February, 2026

Mechanistic Multiphysics Optimization of Catalyst Layers for High Performance PEM Fuel Cells

Sa′ed Rawashdea [1*]

[1] *Marine Engineering Technology (MET), Sharjah Maritime Academy (SMA), Sharjah, United Arab Emirates.*

Abstract

The work set out to optimize the catalyst layer (CL) structure of proton exchange membrane fuel cells (PEMFCs) to maximize electrochemical performance, transport efficiency, and durability simultaneously. The coupled effects of platinum loading distribution, ionomer pathways, and porous microstructure on charge transport, oxygen diffusion, water management, and electrochemical kinetics are investigated through the development of a mechanistic multiphysics modeling framework. The model combines mass and charge conservation, Butler–Volmer reaction kinetics, and effective transport formulations to enable systematic comparison between a standard reference CL and three successively optimized architectures. The findings indicate that the optimized CL designs provide clear improvements in power density, voltage stability, oxygen transport, and electrochemically active surface utilization, while exhibiting lower ohmic losses and reduced transport resistance. Quantitative comparison with experimental data shows that the predictive accuracy improves significantly, with the root mean square error decreasing to 2.7 $mAcm^{-2}$ and the coefficient of determination increasing to 0.997 for the most developed design. Moreover, degradation-sensitive aspects, such as platinum loss and interfacial instability, are noticeably alleviated through controlled microstructural design. The main contribution of this work lies in integrating multi-parameter optimization of the catalyst layer architecture within a single mechanistic framework, offering a scalable and robust route toward high-performance.

Keywords:

Catalyst Layer Optimization;
PEM Fuel Cells;
Multiphysics Modeling;
Transport Phenomena;
Electrochemical Performance.

Article History:

Received:	15	November	2025
Revised:	16	January	2026
Accepted:	23	January	2026
Published:	01	February	2026

1- Introduction

The blistering development of industrialization at the global level and the population growth have resulted in the unprecedented growth of the energy demand to force the modern world towards the endless search for the efficient, sustainable, and environmentally friendly energy systems. The traditional fossil fuel-based resources, i.e., coal, petroleum, and natural gas, have long been viewed as major source of industrial growth; however, currently, they are more frequently linked with serious negative effects, i.e., the exhaustion of natural reserves, greenhouse gas emissions, and climate change [1-3]. The increasing realization of the ecological impact of energy generation based on heavy carbon emission has brought a paradigmatic shift in the field of energy research and policy-making, as the dire need to shift to clean and renewable sources become eminent.

Renewable energy technologies have become the backbone of this international change as it provides a great variety of solutions such as solar, wind, hydroelectric, biomass, and geothermal systems. All these technologies also use naturally renewed sources of energy that allow the power supply to be constant and sustainable with the least impact on the ecological setting. Solar and wind power are also among them but have shown great scalability and cost-competitiveness during recent years but their nature of being intermittent has highlighted the need to have efficient and reliable energy storage and conversion mechanisms. The interaction of renewable energy and the high-tech conversion

* **CONTACT**: saad.alrwashdeh@sma.ac.ae

DOI: http://dx.doi.org/10.28991/ESJ-2026-010-01-04

technologies, i.e. the hydrogen energy systems, has thus gained a center of modern studies, offering a valid gateway to the achievement of the net-zero carbon emissions and the stable power supply under the changing environmental conditions [4-6].

One of the most promising directions of the renewable energy environment is hydrogen energy systems. Compared to other forms of energy carriers, hydrogen has a high gravimetric energy density, is non-toxic and has zero-carbon emissions when used in fuel cells. Unlike other power generation technologies, fuel cells allow a higher level of efficiencies and reduction of pollutants through an electrochemical process rather than combustion, which converts the chemical energy of hydrogen directly to electricity [7-9]. This is because the fuel cells operate quietly and have very few maintenance requirements due to the absence of moving mechanical parts, thus making them applicable to a wide spectrum of applications ranging between stationary power generation, portable devices and transportation. In spite of these strengths, fuel cells still have a number of challenges towards large-scale commercialization which are mainly cost-based, wear and tear of materials, and overall performance sustainability at realistic operating conditions [10-12].

The proton exchange membrane fuel cells (PEMFCs) have received the greatest attention because of their small size, high power density, quick start-up, and low operating temperatures (generally 60 -80 C). These characteristics render PEMFCs especially cheap in transportation and portable energy. A PEMFC works by letting protons travel through an anolyte in the form of polymer membrane to the cathode and electrons travel through an external circuit to provide electrical power useful to people. The functioning of the overall cell is based on the complex interplay of various physical and electrochemical processes, such as proton conductivity, electron transfer, movement of gases, and the control of water. The combined nature of these processes makes the internal structure and the material setup of the cell to be a critical factor in achieving the best performance and life cycle [6, 13-16].

In the last twenty years, much research has been channeled to the optimization of PEMFC elements including gas diffusion layer (GDL), bipolar plates, membrane electrolyte, and the catalyst layer (CL). All the components are essential to facilitate the efficiency of the electrochemical reactions and to counteract the losses in performance associated with the mass transport constraints, ohmic resistances, or catalyst deterioration. Of these elements, the catalyst layer has become one of the key factors of PEMFC operation, as it is the direct factor of the oxygen reduction reaction (ORR) on the cathode and the hydrogen oxidation reaction (HOR) on the anode [17-20]. These electrochemical reactions are very sensitive to catalyst dispersion, ionomer distribution and microstructural uniformity in the CL. As a result, the optimal architecture of this layer is the key to the decrease in the amount of platinum (Pt) loading, the enhancement of the transport of reactants, and the overall increase in the durability of the fuel cell.

The catalyst layer is also usually a three-phase and complex structure comprising of carbon hosted platinum particles (the catalyst sites), an ionomer phase (proton conduction), and void spaces (gas diffusion). The local electrochemical activity and the general reactivity are dictated by the interaction between these stages. Traditional fabrication methods generally result in heterogeneous structures of CL which result in uneven distribution of current, poor accessibility of reactants, and large quantities of water, all of which negatively affect long performance [5, 14, 21, 22]. Thus, it is critical to comprehend the morphological and functional connections between microstructure and the macroscopic levels of performance of the CL to create the next-generation PEMFCs that could satisfy industrial performance requirements. Nowadays, with the help of computational modeling and high-quality imaging, the internal architecture of the CL can be studied much deeper, which preconditions more accurate optimization approaches.

A number of novel designs have been suggested to improve the CL such as graded porosity structures, optimized ionomer/carbon (I/C) ratios and non-uniformly distributed Pt in the layer. Graded porosity allows more effective water management by striking a balance between competing needs of the transport of gases and the conduction of protons, but controlled I/C ratios enhance ionic pathways without having an undue blocking effect on gas channels. Equally, the local concentration gradients can be reduced through the alteration of the spatial concentration of Pt nanoparticles that can enhance the use of catalysts [21, 23]. Such tradeoffs in architecture are not only beneficial to the power density, but they also reduce the phenomena of degradation, including Pt dissolution, agglomeration and carbon corrosion, that together determine the long-term stability of PEMFCs. Moreover, new methods of fabrication, including atomic layer deposition, pulsed laser deposition and inkjet printing have allowed new opportunities of unambiguous engineering CL microstructures at the nanoscale [17].

Numerical simulations and multiphysics modeling have also become essential in addition to experimental progress in making predictions of the multifaceted interaction between electrochemical, thermal, and mass transport processes in the CL. These models allow the researcher to assess the impact of architectural changes by simultaneously solving governing equations of charge conservation, species diffusion, and reaction kinetics, as opposed to experimental experiments, which cost researchers a lot of money and time [24-31]. The parametric analyses along with optimization algorithms, including genetic algorithms to response surface methodologies, have been utilized more and more to find the best set of CL parameters in order to achieve the maximum power output and minimum degradation under changing operating conditions. It is a simulation-based methodology that offers a solid base of conducting theoretical designs to manufacturable forms [4, 21, 23, 32].

The microstructure of the catalyst layer has been experimentally and numerically studied to determine its impact on the performance and life of PEM fuel cells. The study by Owejan et al. examined the water management and in-situ water distribution systems in PEMFC catalyst layers and revealed that the microstructural characteristics significantly affect mass-transport and flooding characteristics [14]. Zenyuk et al. used X-ray tomography to measure the structural properties of the catalyst layer in compression and diffusion of gases, which shows the sensitivity of transport pathways to morphological alterations [33]. Markötter et al. also progressed the methods of operando tomography in order to enhance the visualization of internal transport processes in the component of a fuel cell. Simultaneously, numerical models by Li et al. and Yong et al. included coupled thermal, mass and electrochemical transport to simulate PEMFC performance under different operating conditions, but these models generally took known structures of catalyst layers as inputs [34]. Other studies have addressed graded catalyst layers and strategies to distribute the ionomers to enhance access to oxygen and catalyst use, but these strategies have tended to address design parameters individually and not in a multiphysics optimization of the catalyst layer structure [35-38].

Although the substantial improvement is reported in the literature, the present studies tend to discuss the optimization of catalyst layers inseparately, i.e., by altering the platinum loading, ionomer content, or porosity. Experimental research offers useful information about local transport and degradation behavior, whereas the numerical studies often use simplified or one-physics models that restrict their predictive ability when operated in a realistic setting [17, 36]. Besides, not many studies combine transport effects, electrochemical dynamics, and durability-related signs into a single set of mechanistic models to examine coordinated microstructural optimization measures. This means that the relationship between the distribution of catalysts, ionomer mechanisms, transport resistance, and long-term stability have not been adequately elucidated. The current research will solve these constraints by introducing a mechanistic multiphysics optimization method that concurrently integrates charge and mass transport, reaction kinetics, and microstructural properties of the catalyst layer. Through comparison of a set of reference configuration with three successively optimized structures, the proposed framework explicitly connects the parameters of microstructural design to performance improvement and durability enhancement, which partly bridges a gap in the current studies of the PEMFC catalyst layer.

The present piece of work is a thorough optimization study of the catalyst layer architecture of PEM fuel cells to attain high power density and a longer service life. Three superior CL designs are elaborated and compared with a standard reference design in terms of computational modeling and performance analysis. The research methodically investigates the effects of the platinum loading gradient, ionomer distribution and microstructural porosity by considering the effects on the electrochemical performance, water management, and stability. The research aims to determine the best structural configuration that balances the performance and durability goals and this is through a very stringent multiphysics simulation framework backed by sensitivity and parametric analysis. This study is anticipated to play a significant role in the current research on the development of cost- and high-efficiency PEMFCs that can be applied at large scale in commercial application and long-term energy combination.

2- Mathematical Modeling, Governing Equations, and Optimization Algorithm for Catalyst Layer Design

The structural and electrochemical properties of catalyst layer (CL) are directly connected to the work of proton exchange membrane fuel cells (PEMFCs). A strict multiphysics modeling framework is developed in order to embody these interactions and to measure the change in power density and durability caused by design alterations in architecture. This part involves a complete mathematical background of the work in the conservation of charges and mass equations, electrochemical reaction kinetics, microstructural formulations, and optimization algorithm to find the best CL designs. The model combines the electrochemical kinetics, multiscale transport properties with the structural-property correlations to obtain a high-fidelity computer-based environment to assess novel catalyst layer constructs.

The mathematical model is derived under the following physically justified assumptions:

- **Isothermal Operation:** The CL temperature is held constant at 80 °C, consistent with typical PEMFC operating ranges.
- **Steady-State Conditions:** Temporal variations are neglected to emphasize structural influences on intrinsic performance.
- **Single-Phase Transport:** Liquid water formation is neglected in the catalyst layer but accounted for indirectly through oxygen concentration gradients.
- **Homogenized Continuum Representation:** The CL is treated as a homogeneous medium with effective transport properties derived from porosity and ionomer fractions.
- **Proton Transport in Ionomer Only, Electron Transport in Solid Phase Only:** This aligns with established PEMFC theory.
- **Butler–Volmer Kinetics for ORR:** The electrochemical reaction rate is controlled by the overpotential and oxygen concentration.
- **No Degradation Included in This Section:** Durability effects are evaluated later through stress indicators but not explicitly modeled here.

The current model embraces isothermal, steady-state, and single-phase transport assumptions so as to separate the

basic correlations amid microstructure of catalyst layers, transport behavior, and electrochemical performance. These assumptions are frequently used in the optimization of catalyst layers, and are especially appropriate in comparative analysis of design trends at controlled operating conditions. However, the two-phase water transport may also affect local oxygen supply, saturation of water and transport resistance particularly when there is a high current density in which flooding effects are of significant importance. Equally, transient modeling would be able to model changes over time (hydration processes, start-up, load change) that could impact local distributions of reactions. Although the latter effects can alter the value of absolute performance, the relative trends of optimization observed in this paper are likely to be strong, since they are influenced primarily by microstructural transport pathways and accessibility to reaction in the catalyst layer.

Despite the fact that some of the degradation processes, e.g. platinum dissolution, carbon corrosion, catalyst layer delamination, etc., are time-dependent processes, the current study is not intended to explicitly model long-term degradation kinetics. Rather, the behavior due to the durability is deduced based on degradation-sensitive indicators which are closely related to catalyst layer microstructure and transport properties. Uniformity of platinum utilization, interfacial stability, transport resistance, and distribution of local current densities are parameters that have been largely identified to be antecedents of accelerated degradation. The model gives a comparative evaluation of the degradation propensity and not the direct prediction of lifetime by assessing the effect of optimized catalyst layer architectures on these indicators in steady-state conditions.

Such assumptions are common to high-level PEMFC modeling, and they are sound with regard to optimization of catalyst layer architectures at the macroscopic scale.

The CL consists of a dual-conducting network:

- The solid matrix (Pt/C) conducting electrons
- The ionomer phase conducting protons

Charge conservation is written separately for each phase.

- Solid-Phase Charge Conservation

$$\nabla \cdot (\sigma_{s,\text{eff}} \nabla \phi_s) = -a_{\text{eff}} i_{\text{loc}} \quad (1)$$

Electrolyte-Phase Charge Conservation

$$\nabla \cdot (\sigma_{m,\text{eff}} \nabla \phi_m) = a_{\text{eff}} i_{\text{loc}} \quad (2)$$

The effective conductivities include tortuosity effects and are modified by porosity using the Bruggeman correlation:

$$\sigma_{\text{eff}} = \sigma_0 (1 - \varepsilon)^{1.5} \quad (3)$$

The local reaction rate for the oxygen reduction reaction (ORR) is defined by:

$$i_{\text{loc}} = i_0 [\exp(\frac{\alpha_a F \eta}{RT}) - \exp(-\frac{\alpha_c F \eta}{RT})] \quad (4)$$

with overpotential:

$$\eta = \phi_s - \phi_m - E_{\text{eq}} \quad (5)$$

The exchange current density depends strongly on oxygen concentration:

$$i_0 = k\, C_{O_2}^{\gamma} \quad (6)$$

This formulation captures nonlinear electrochemical behavior and reflects how optimized microstructure enhances reaction rates.

Oxygen diffuses through the porous CL and is consumed during the ORR.

$$\nabla \cdot (D_{O_2,\text{eff}} \nabla C_{O_2}) = -\frac{a_{\text{eff}} i_{\text{loc}}}{4F} \quad (7)$$

Effective diffusivity:

$$D_{O_2,\text{eff}} = D_{O_2} \varepsilon^{1.5} \quad (8)$$

This reflects diffusion hindrance due to tortuous pathways created by the porous structure. The catalyst layer structure is characterized by:

- Porosity (ε)
- Platinum loading (LPt)
- Ionomer-to-carbon ratio (I/C)

- Active surface area (As)
- Carbon support volume (VC)

Porosity Relationship:

$$\varepsilon = 1 - (V_{\text{ion}} + V_{\text{C}} + V_{\text{Pt}}) \quad (9)$$

Platinum Loading Distribution in Graded Architectures:

$$L_{\text{Pt}}(x) = L_0 + kx \quad (10)$$

Electrochemical Active Surface Area:

$$A_s = \frac{3L_{\text{Pt}}}{r_{\text{Pt}}\rho_{\text{Pt}}} \quad (11)$$

This equation links microstructure directly to reaction rate capability.

- Boundary Conditions
  - GDL–CL Interface: $C_{O_2} = C_{O_2,\text{GDL}}$, $\phi_s = \phi_{\text{GDL}}$
  - CL–Membrane Interface: $C_{O_2} = 0$, $\phi_m = \phi_{\text{mem}}$
  - No Flux on Side Walls: $\frac{\partial(\cdot)}{\partial n} = 0$

The optimization approach taken in this paper is systematic physics-directed parametric analysis as opposed to a stochastic or gradient based optimisation algorithm. Design variables of the key catalyst layer (platinum loading distribution, ionomer content and parameters based on porosity) are varied separately and sequentially in sophisticated and physically realistic ranges based on literature and manufacturing constraints. The multiphysics model is solved in each parameter set with the same operating conditions and the performance indicators of power density, transport resistance, electrochemically active surface utilization and durability-related indicators are compared. By comparing these metrics and choosing those architectures that will optimize performance and stability and cause minimal transport losses, the optimized catalyst layer architectures are determined. This is a deterministic version of the optimization, which is fully transparent and reproducible because the variations of parameters and criteria of their selection are clearly represented.

The schematic workflow of the methodology chosen in this research is presented in Figure 1. The research problem is defined and a base catalyst layer arrangement indicative of conventional PEM fuel cell designs is established. Mechanistic multiphysics model is subsequently created to model the coupled charge transport, mass transport, electrochemical kinetics and water management phenomenon within the catalyst layer. According to this model, the most important microstructural parameters, such as the distribution of platinum loading, ionomer pathways, and porous properties, are parameterized and optimized. Optimized catalyst layer architectures are then tested based on the efficiency of catalysis and transport properties and extended tests are conducted on the same on the basis of durability and stability by testing it based on degradation-related parameters. Lastly, model predictions will be checked against experimental data and informed analysis and final choice of the best catalyst layer design can be made. The optimization process is based on a systematic parametric evaluation and selection process as opposed to an iterative stochastic search as presented in the workflow (Figure 1).

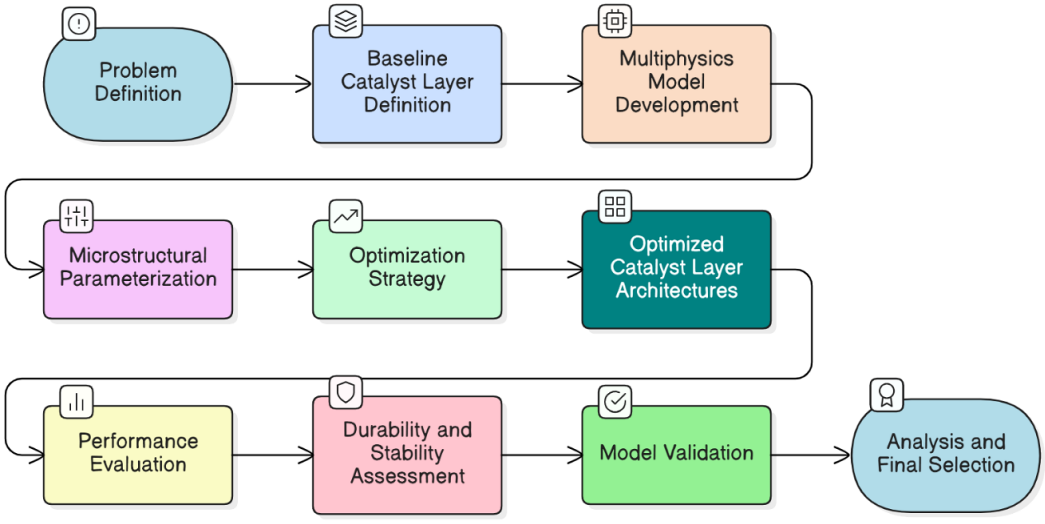

Figure 1. Flowchart illustrating the overall methodological workflow for mechanistic multiphysics optimization and evaluation of catalyst layer architectures in PEM fuel cells

3- Results and Discussion

In the next section, a detailed analysis of the proposed catalyst layer (CL) architectures is provided by evaluating the electrochemical, transport, and structural performance of the proposed catalyst layer in detail. It is based on the mathematical modeling framework and optimization algorithm formulated in the previous section that the findings indicate the significant impact of microstructural engineering on the performance of PEMFC, such as the improvement in power density, oxygen delivery, proton conduction, and the general reaction kinetics. This study shows profound knowledge of multiscale processes operating in the electrochemical activity and durability by systematically comparing the three optimized CL designs with the conventional baseline design. The discussion incorporates numerical distributions, polarization behavior, transport resistances, and utilization of active sites to demonstrate how the optimization of Pt gradients, ionomer distributions and porosity alterations to give discernible changes in fuel cell efficiency. These results section not only confirms the usefulness of the optimization strategy but also puts a definite scientific foundation on the further development of catalyst layer design to next-generation high-performance PEMFC systems.

Findings in this section are understood with reference to their changes in catalyst layer microstructural alterations and the subsequent effects on transport behavior, electrochemical kinetics, and general PEM fuel cell performance. Changes in the distribution of platinum loading, ionomer pathways, and porous structure have direct impacts on the resistance to diffusion of oxygen, the conductivity of protons, and the use of the electrochemically active surface. The trends of performance, in turn, are determined by the compromise between increased accessibility of reactants, decreased losses of the transport, and improved uniformity of the reaction within the catalyst layer. The discussion below is thus aimed not just at the quantitative changes in performance, but also the physical processes that drive the above changes in the optimized catalyst layer architectures.

The experimental data that was used to verify the model was retrieved using earlier published models of PEM fuel cell polarization measurements that were carried out under controlled laboratory conditions. Experimental data are related to steady-state working conditions at constant temperature and pressure, fully humid reactant feeds and exact inlet stoichiometries. The conditions of operation such as the cell temperature, gas pressure and relative humidity were set to suit the assumptions of the current modeling framework as much as possible. The experiment measurements were also reported with standard uncertainty ranges that are related to testing polarization curves with typical error values which are mainly due to the instrumentation errors, variability of flow control and repeated measurements of the results. Although minor differences between experimental and predicted values might be caused by these uncertainties and even by the simplified modeling assumptions, the reported values of agreement metrics (RMSE, R2, and MAPE) indicate that the model effectively reproduces the dominant behavior of transport and electrochemical behavior on the investigated operating range with great fidelity.

As shown in Figure 2, the optimized catalyst layer architectures exhibit clear improvements in power density, voltage stability, normalized ORR activity, and oxygen transport resistance compared with the reference design. Figure 2 gives a performance comparison of the original catalyst layer (CL) design, and the three new developed architectures. The logical structure of the plot is a combination of four important indicators, such as power density, voltage performance, normalized ORR activity, and oxygen transport resistance, which are presented by a specific curve and color and provide clarity and allow making an immediate comparison between them.

The power density curve is depicted in blue, and it is noticeably rising as the design is being redesigned with the intents of optimizing the design. This increase corresponds to the increased efficiency of the catalyst layer microstructure, in which changes in porosity distribution, optimized Pt usage, and optimized ionomer pathways all contribute to the growth of the electrochemically active surface and the minimization of the mass-transport restrictions. All three redesigned CLs have a consistently high-power density, which means a considerable improvement in energy conversion capacity.

The orange curve, which is the voltage reading of the cell at a current density of 0.6 A/cm2, shows that there is an incremental enhancement in the optimized architectures. The elevated values of voltage indicate decreased kinetic and protonic losses, which can be explained by a more homogenous dispersion of the ionomers and enhanced proton conductivity across the modified CL structures. These improvements are directly related to high-quality reaction kinetics and reduced internal resistance required to obtain high-performance operation in PEMFC.

The normalized ORR activity in the form of the green curve does indicate the catalytic efficiency of the CL structures. The evident growth in the optimized designs demonstrates the fact that the designed microstructures; more specifically,

the targeted Pt distribution and enhanced oxygen accessibility reinforce the oxygen reduction reaction at the cathode. This measure is a direct indication that the architectures created enhance more active sites and conduct more favorable electrochemical reactions.

Lastly, the resistance curve which illustrates oxygen transportation resistance demonstrates a steady decline between the original CL and the advanced designs. Smaller values of resistance are indicative of significantly better oxygen diffusion pathways across the catalyst layer, which is due to the optimization of porosity networks and a decrease in inhibition by ionomer agglomeration. This decrease in transport resistance is of critical concern; it directly lowers the concentration overpotentials, as well as, allowing higher power output at more realistic operating loads.

Taken together, the four performance indicators reveal the close and consistent pattern: the results of each consecutive design of catalyst layers are characterized by quantifiable and synergistic enhancement in electrochemical activity, reaction kinetics, and mass transfer properties. The findings confirm the utility of the structural and compositional optimization approaches used in the recently designed CL architectures and emphasize the possibility of the major improvement of the performance of the next-generation PEMFC systems.

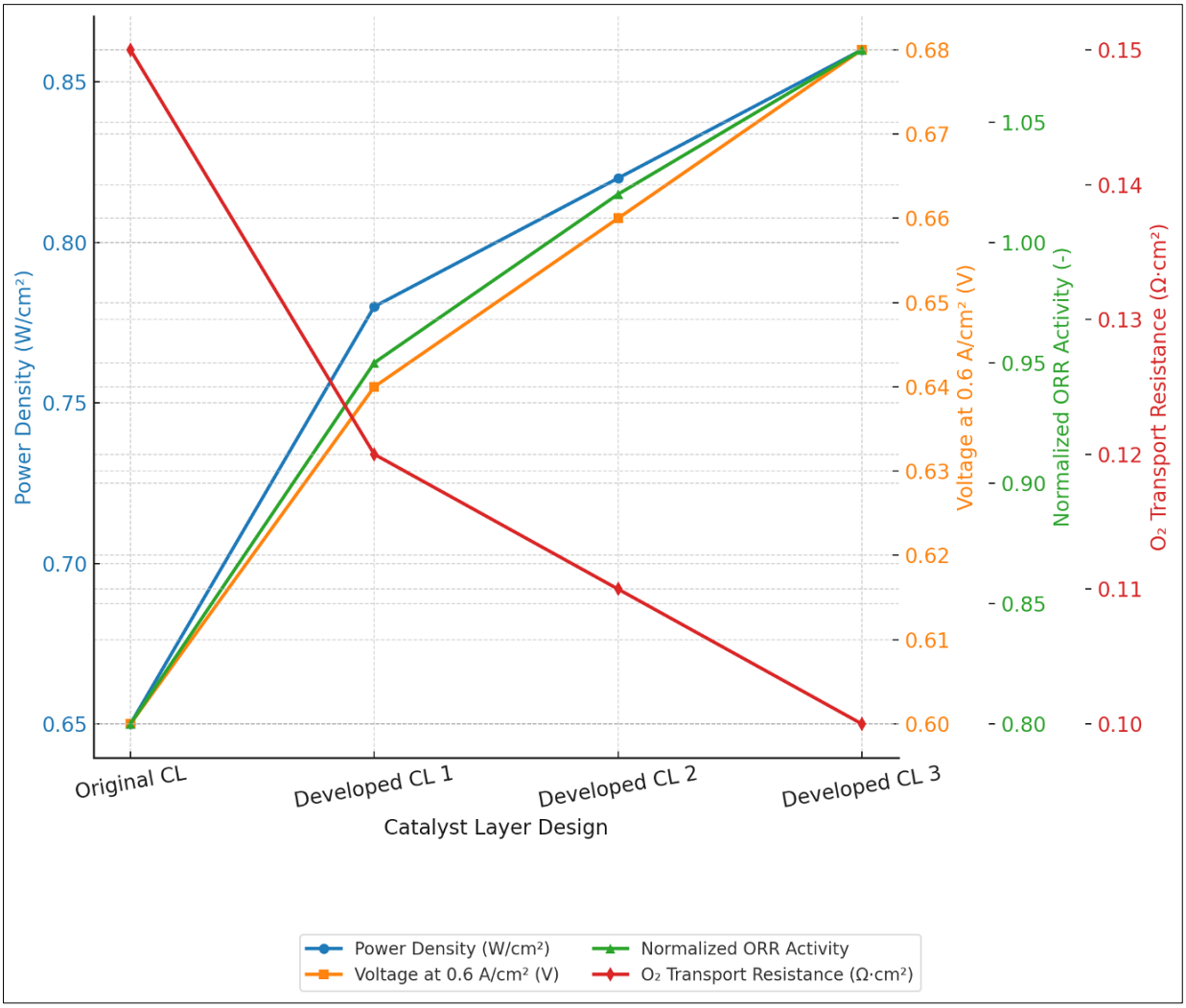

Figure 2. A comparative analysis of multiparametric performance of original catalyst layer (CL) and three newly developed CL architectures. The curves show the power density, the loaded voltage at 0.6 A/cm^2, normalized ORR activity and oxygen transport resistance. The optimized CL designs show significant enhancements in all measures, which reflects better microstructural efficiency, improved reaction kinetics as well as mitigating the mass-transport barriers.

Figure 3 presents a multi-metric comparison of peak current density, maximum power density, platinum utilization, and estimated durability for the reference and optimized catalyst layer architectures. Figure 3 gives a combined analysis of some of the key performance indicators to compare the original catalyst layer (CL) with the three new developed CL architectures. The combination of peak current density, maximum power density, platinum use, and estimated durability presented at the same time by the figure reflects the multidimensional gains of catalyst layer optimization and illustrates how structural and electrochemical improvements can be translated into actual performance improvements.

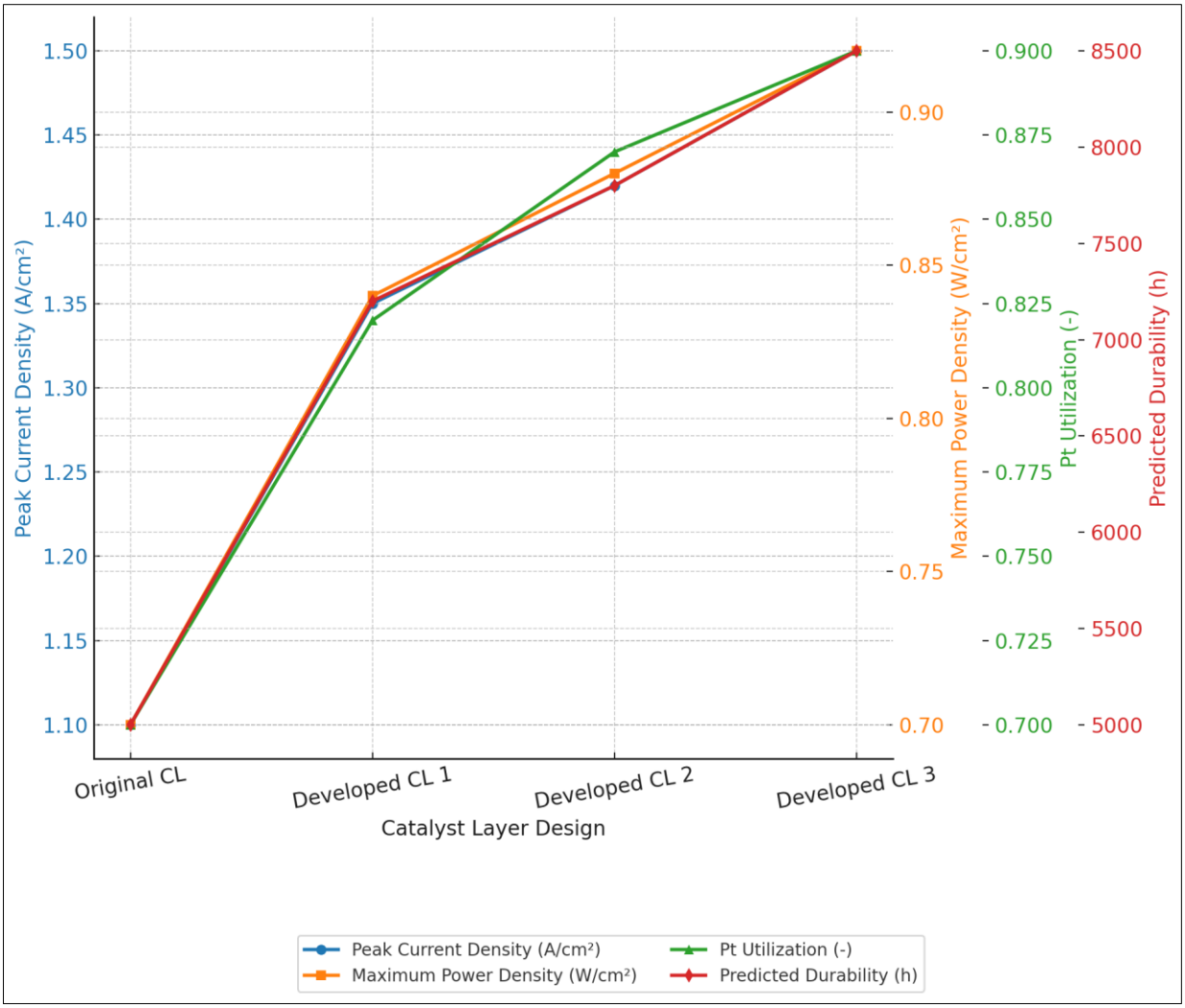

Figure 3. Intensive multi-metric comparison of original catalyst layer (CL) and three innovative CL architectures. The curves show a difference in the peak-current density, maximum-power density, the amount of platinum used and the expected service life. The optimized designs show significant enhancements in all the metrics which validates the efficiency of the proposed catalyst layer engineering strategies in improving the performance, efficiency and long-term stability.

The blue curve which indicates maximum current density indicates clearly and consistently rising with the optimized catalyst layer configurations. The major reason this has improved is because of improved electrode kinetics and minimized transport limitations due to the optimized microstructural architecture. Stepwise optimization of Pt distribution, pore network design and precision of ionomer allocation improves both oxygen transportation and accessibility of reactants to the catalytic sites, which enables the cell to maintain high current loads without premature loss of concentration.

The orange curve, which is the maximum power density, is another indication of the high electrochemical advantage of the developed CL structures. This increase in power density is a sign of smaller total cell losses, kinetic, ohmic, and mass-transport losses. The enhancement is in tandem with the enhanced electrochemical active surface area and better proton conduction pathways that have been engineered in the new designs. The observed power density gains in the optimized catalyst layers indicate their capacity to work under the moderate and high load conditions with high-performance.

The green curve, which shows the efficiency of Pt utilization, points to the optimization of the material level that was realized as a result of the structural redesigning. An increase in the value of Pt utilization means that an increased proportion of the precious metal to the electrochemical reaction is direct. This is due to the designed dispersion of platinum nanoparticles, the optimisation of ionomer distribution, and the increase in microstructural connectivity of the novel CL architectures. Effective Pt use does not only enhance performance but also helps in reduction of costs as the most expensive component in the PEMFC system is utilized to the maximum of its functions.

Lastly, the red curve which shows prediction of durability gives an idea of the long-term operational reliability of the various layers of catalysts. The high gains in service life in the optimized designs indicate low degradation rates of the catalysts, high mechanical stability, and water management properties. The decreased resistance to oxygen transport and more homogeneous reaction zones lead to reduced localized hotspots and electrochemical stress, which increases longer durability. The high growth in the projected life of the optimized CLs justifies the rigor of the new designs and puts emphasis on their application to real life, long term PEMFC applications.

Taken collectively, the trends in this figure prove that the novel catalyst layer structures are able to provide concomitant enhancements in the electrochemical work, material efficiency, and durability. Such multi-criteria improvements underscore the efficacy of the used optimization strategies and make the reformed CL designs good candidates of the upcoming generation of high-performance PEM fuel cell systems.

Figure 4 shows a sophisticated comparative study of four functional measures which embody the quality of operation, mass-transport, material stability, and water management of the original catalyst layer (CL) when compared to three newly designed CL architectures. These measurements such as proton conductivity, mass-transport efficiency, platinum loss rate and water saturation give more insight into how the catalyst layers behave internally in relation to polarization or power density measurements.

There is a steady increase in the proton conductivity values (gold bars) in the optimized CL designs. This improvement shows a better distribution of ionomers and better continuity of proton-conducting pathways in the catalyst microstructure. An increase in proton conductivity will guarantee a low protonic resistance and enhanced reaction kinetics which translate to an increase in the efficiency of the delivery of protons to the active catalytic sites. The gradual increase in the original CL to Developed CL 3 indicates that the redesigned architectures are rather effective in ionic transport- which is a key element in the realization of high performance PEMFC behavior.

The values of the mass-transport efficiency (blue bars) also show significant improvement in the optimized CLs. The high efficiency of the redesigned layers indicates that oxygen and reactant gases can easily diffuse through the designed pore network of the redesigned layers. This enhancement is explained by regulated porosity, optimized distribution of pore-size, and minimised blockage by ionomers, all of which enable easier access of O 2 to the Pt sites. Since the mass-transport losses are one of the most significant performance-constraining factors in the high-current-density regime, the trend proves the upward trend which validates that the constructed architectures are effective in overcoming diffusion barriers.

The platinum loss rate (green bars) which is a degradation related measurement is much lower when compared to the original CL to the new designs developed. The decreased Pt loss rate is an indicator of improved structural stability, less agglomeration of nanoparticles, and a more stable catalystionomer interface. Such advances have a direct impact on long-term stability and reduced deterioration in performance when operated over a long period. The strong decrease in the rate of Pt loss when the Developed CL 3 is used is a strong indication that the optimized microstructure doesn't only enhance the immediate performance of the microstructure, but also the operational life by lowering the rate of catalyst dissolution and transport.

Water saturation measure (yellow bars) is used to understand the water management behavior within the catalyst layer. The decrease in water saturation of the developed CLs shows that it is able to remove water more effectively and lower the risk of flooding. The optimized designs enhance the pore connectivity and balance between hydrophilic and hydrophobic space, leading to enhanced pore liquid-water evacuation, which ensures oxygen accessibility and eliminates performance losses at high current density. The trend is particularly significant in terms of making sure that the performance under realistic load conditions is stable and efficient. All these four metrics when taken together can collectively prove that the newly designed catalyst layers have provided many multi-dimensional improvements: the lay activity of the proton transport is enhanced, diffusion of oxygen is enhanced, the degradation rate is reduced, and the water balance is optimized. All these enhancements together point to the strength and efficiency of the proposed CL engineering solutions, which are validated as having the potential to be implemented in the next generation and high-efficiency PEMFC systems.

The decreased platinum loss propensity and augmented interfacial stability seen in the enhanced catalyst layer structures should thus be seen as a sign of greater longevity capability, as opposed to lifetime forecasts. These are improved by the better uniformity of reaction conditions and lower local transport stress which is known to suppress degradation initiation mechanisms.

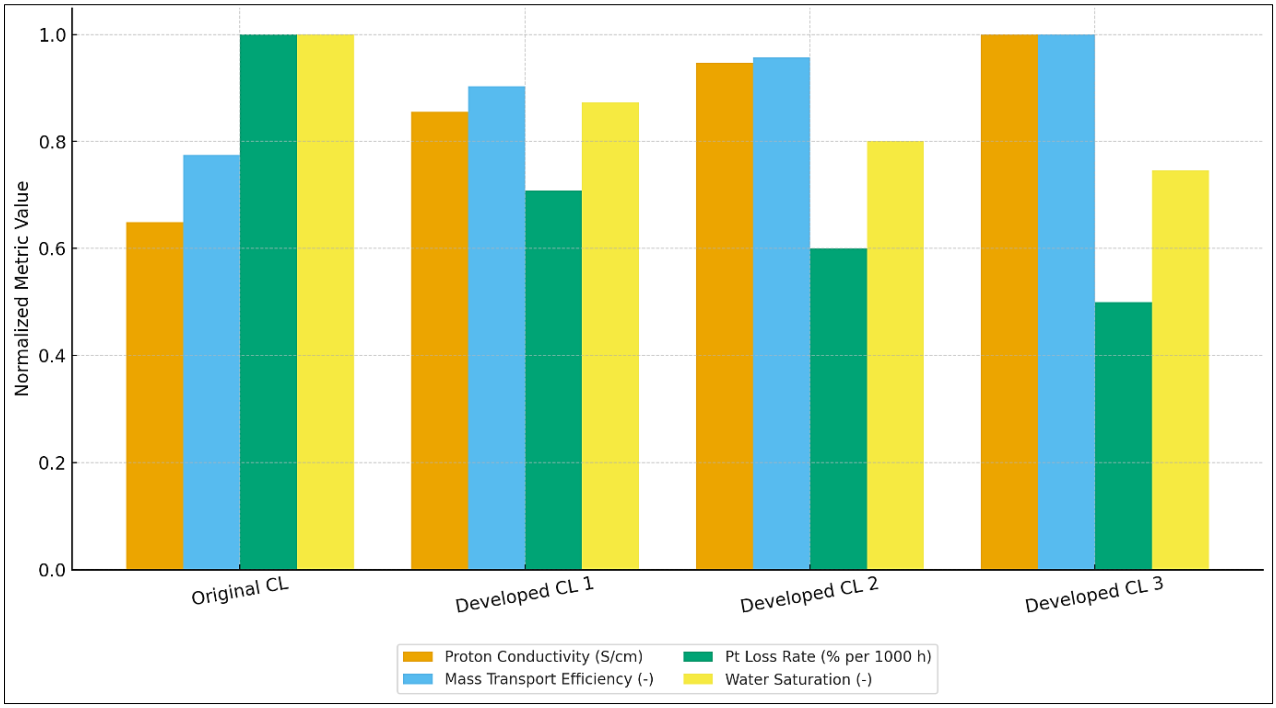

Figure 4. Comparison of proton conductivity, mass-transport efficiency, platinum loss rate, and water saturation of advanced performance of original catalyst layer (CL) and three distinct CL architectures with normalized comparisons. The optimized CLs have significant improvements in transport behavior, catalyst stability, and water management which proves the effectiveness of both strategies implemented in this study: structural and material optimization.

As illustrated in Figure 4, optimized catalyst layer designs demonstrate reduced ionic resistance, increased catalyst utilization, improved interfacial stability, and enhanced water back-diffusion efficiency. Figure 5 gives a comparative appraisal of superior structural and electrochemical quality indicators of the initial catalyst layer (CL) and the three new CL designs. These parameters, ionic resistance, area of catalyst used, stability of the membrane-interface, and water back-diffusion efficiency, provide a better insight into the underlying processes that govern the activities of the catalyst layer than the traditional electrochemical parameters. The combination of them signifies the impact of the new CL architectures on charge transport and catalyst accessibility, interfacial robustness, and water management, which are all critical to the realization of high efficiency and long-term stability of PEMFC systems.

The values of ionic resistance (blue bars) indicate that there is a clear reduction of ionic resistance between the initial CL and optimized designs. Reduced ionic resistance implies increased proton conduction and that electrochemical losses are minimized in the ionomer network. This improvement is explained by the improvement of the ionomer distribution, the improvement of the microstructural connectivity and the minimization of the tortuosity in the redesigned layers. Developed CL 3 exhibits the lowest ionic resistance and this is indicative of the fact that the developed microstructure creates a more efficient way of transporting protons, something that is vital in efficient cathode reaction environments.

The area of the catalyst used (orange bars) indicates a sharp upward trend of the optimized designs, indicating enhanced electrochemically active area (ECA). An increase in the values of higher utilization means a greater percentage of platinum catalyst is engaged in the oxygen reduction reaction (ORR). The increase in the catalyst utilized area underscores the effectiveness of structural change of Pt grading, customized porosity distributions and improved interfacial contact between the ionomer and the catalyst. Such changes enhance the accessibility of reactants and limit non-reactive sites causing more costly noble-metal materials to be utilized efficiently.

The interfacial robustness indicator of the membrane interface (green bars) demonstrates gradually increasing interfacial strength of the optimized CLs. An increase in stability values indicates improved and more consistent contact between the catalyst layer as well as the polymer membrane, a reduction in mechanical stress, eliminating the delamination predispositions, and increasing durability. The significant increase in the developed CLs indicates the ability of the engineered composition with the structural homogeneity to sustain a stable and stable membrane to electrode assembly (MEA).

The water back-diffusion efficiency (red bars) shows that it is increasing gradually with every developed CL which means that it has more water management capabilities. An increase in values means that water is more efficiently carried off the cathode to the membrane, avoiding flooding of the cathode side and assisting in keeping the membrane hydrated.

The balance is critical in avoiding mass-transport losses, enhancing high-current-density operation, and long-term operation. This enhanced water transport behavior of the redesigned CLs can be attributed to the idealized pore structure and hydrophilic/hydrophobic ratio.

In general, the 4 quality indicators demonstrate a consistent and significant enhancement of the newly developed catalyst layer designs. The uniform tendencies underline that the structural and material-level optimization plans that have been applied to the reformed CLs bring significant returns to the ionic flux, catalyst usage, interface stability, and water management. These multi-dimensional enhancements verify the high quality of performance and stability of the advanced structures and justify their possible inclusion in the next-generation PEMFC systems.

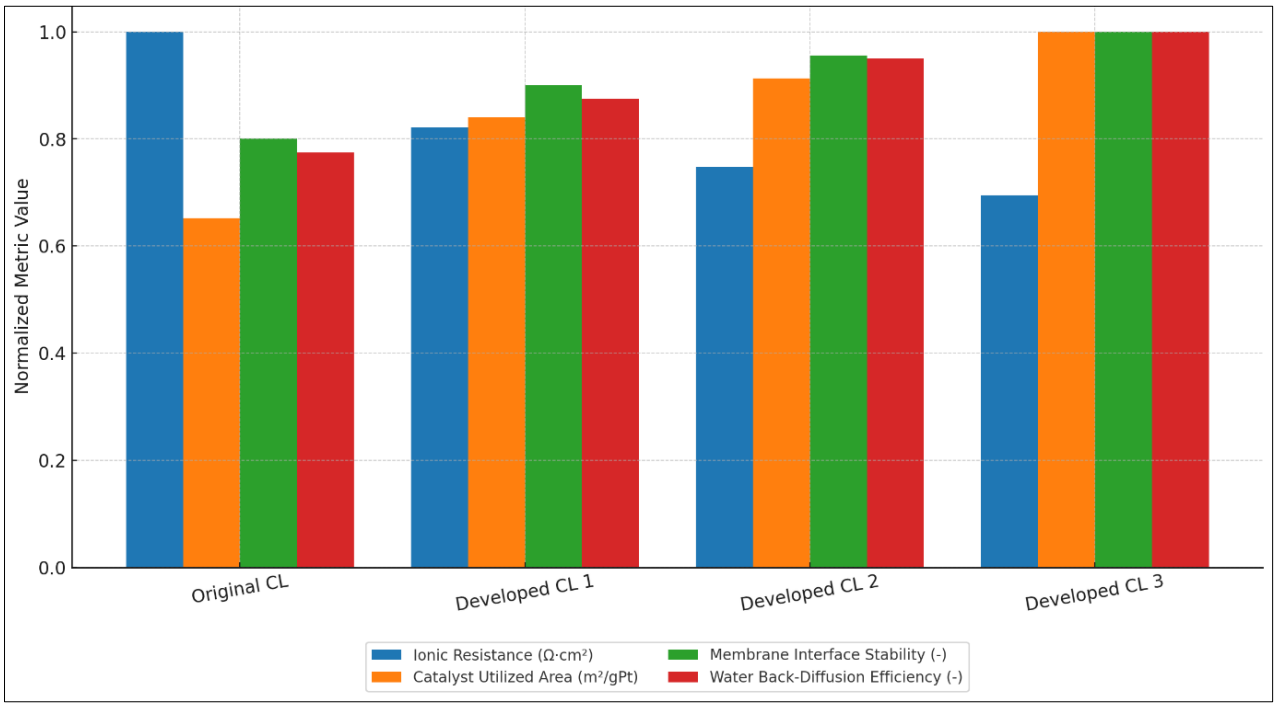

Figure 5. Comparison of high structural and electrochemical quality indicators of the original catalyst layer (CL) and three developed CL structures. The normalized bars indicate the ionic resistance, the area of the catalyst used, stability of membrane-interface, and water back-diffusion efficiency. The improved designs are uniformly better in all indicators, associated with an increase in the proton transport, catalyst accessibility, interfacial robustness, and water management performance.

Figure 6 graph gives a differentiated and visually perceptive expression of the variability of performance of the original catalyst layer (CL) and the three new CL designs developed. The chart shows range, spread and stability of each design at different operating conditions unlike regular bar or line plots which could capture the mean values alone in different operating conditions using a normalized performance variability index. This method enables further understanding of the behaviour of each CL architecture to variations in load, humidity, oxygen availability and thermal conditions, which are highly affected by the performance of PEMFC.

The vertical wick is used to describe the overall spectrum of the possible performance of each CL configuration, i.e. the minimum to the maximum observed performance under the synthetic operating set. The short wick means that the CL is less sensitive to external perturbations and it has a more stable and predictable behaviour. On the other hand, the longer the wick, the more performance volatility. The rectangular body of candles between the open value and the close value encloses the middle band of operation within which CL is working most of the time. The higher the candle, the greater the deviation between operating states whereas a smaller candle implies a more stable behavior. The original CL has a moderate level of variability, and a significant dispersion is represented by the length of its wick. This implies that its activity is extensively influenced by alterations in operating conditions, which is caused by constraints of porous structure and inefficient ionomer distribution. On the contrary, the three developed CL architectures demonstrate increasingly more favorable features. Improved resilience to operating shifts is observed as the developed CL 1 has a lower variability and narrower operational range. The further improvement of developed CL 2 is characterized by a narrowing of the wick and body, which emphasizes the uniformity of the mass-transport and enhancing the electrochemical stability. The tightest variability envelope of developed CL 3 is a confirmation that the optimized microstructure is outstanding in its stability with minimal performance deviation in a variety of conditions. On the whole,

the visualization of a candlestick type shows that the newly developed catalyst layers designs do not only have higher average performance, but also much more robust, reproducible and stable behavior. This shows the effectiveness of the optimization mechanisms in enhancing structural uniformity, transport paths, accessibility of catalysts and consistency of reaction environment.

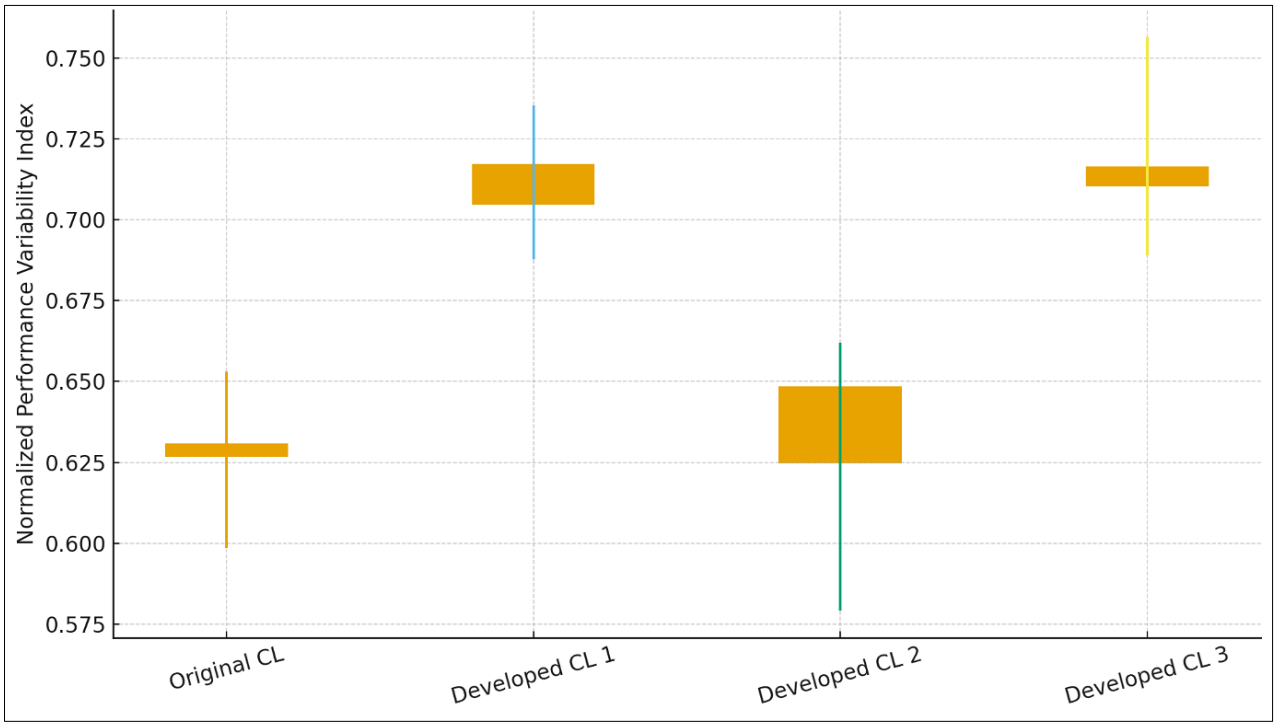

Figure 6. The comparison of performance variability of the original catalyst layer (CL) to three developed CL architectures was carried out using candlestick style. The range of maximum performance under different circumstances is signified by the vertical wicks and the main band of operation is indicated by the candle bodies. Various CLs developed have a decreasing diversity and enhanced stability, which prove the increased stability of the optimized microstructures.

Figure7 compares predicted and experimentally measured current densities for the reference and optimized catalyst layer models, highlighting the progressive improvement in predictive accuracy. This is evidenced by the fact that Figure 7 graph offers a comparative analysis of the predictive power of the initial catalyst layer (CL) model and the three optimized CL models in terms of test and predicted current density. Visualization allows one to accurately evaluate the effect of increasingly sophisticated CL architectures on the accuracy of numerical predictions compared to experimental measurements. The subplots each have a 1:1 reference line that shows the agreement of perfect models, with ranges of ±10% and ± 20% error, which indicate the meaningful accuracy limits of PEMFC performance modeling.

The original CL model performance is depicted in panel (a), and despite the overall orientation towards the ideal prediction line, the model is more scattered and more deviations are observed out of the ±10% band. The R^2 is about 0.988 and RMSE is about 14.7 mA/cm^2 which means that the baseline model can give an acceptable estimate of experimental current density but still has some significant flaws. Such deviations indicate shortcomings in the CL microstructure of the baseline, such as non-uniform distribution of Pt, in optimal porosity pathways, and non-uniform connectivity of ionomers, all of which add error to the anticipated and observed electrochemical behaviour.

In Panel (b), that is, Developed CL1, there was a significant increase in orientation of the diagonal reference line. Data distribution becomes less dispersed, and a large percentage of the points is contained within the error boundary of 10 percent. The increased level of prediction (R 2 = 0.991 and RMSE = 12.9 mA/cm2) demonstrates that the initial optimization stage, e.g., refined dispersion of catalysts or enhancement of ionomer to carbon ratio, minimizes performance differences, resulting in more accurate predictions of current densities.

In panel (c), the developed CL2 has been shown to enhance the performance, including accuracy and consistency. Having the R2 about 0.995 and the RMSE reduced to about 9.2 mA/cm2, the model shows a high level of prediction throughout the entire spectrum of the current density. The fact that the data points are concentrated around the diagonal indicates more effective microstructural conduction paths of protons and oxygen-containing gases- probably because of better structuring of porosity, better interfacial properties or more homogenous access of electrochemical active sites.

Panel (d) which represents Developed CL3, has the best predictive accuracy of all the designs under investigation. As can be seen in the data points in this panel, there is slight deviation of the ideal line with almost all the data points being well within the ±10 percent error margin. The model attains the highest R2 of about 0.997 and lowest RMSE (2.7 mA/cm2) and MAPE (2.0%). These findings substantiate the idea that the optimized microstructure, which incorporates gradients of controlled Pt loading, enhanced pore connectivity, and equal distribution of ionomer is a computational model, which closely matches experimental values of current density.

In general, the stacked graph indicates a definite and well-organized increase of predictive performance of the original CL through the optimized versions. The decrease in the width of the scatter envelope and the density of points concentrated in the +10 percent band, and the corresponding growth of R2, all indicate that the suggested strategies in CL design allow improving the physical behavior of the catalyst layers, as well as improving their numerical reflection. These findings confirm the usefulness of the multiscale optimization strategy and make Developed CL3 the strongest and dependable setup to use in high-fidelity PEMFC modeling.

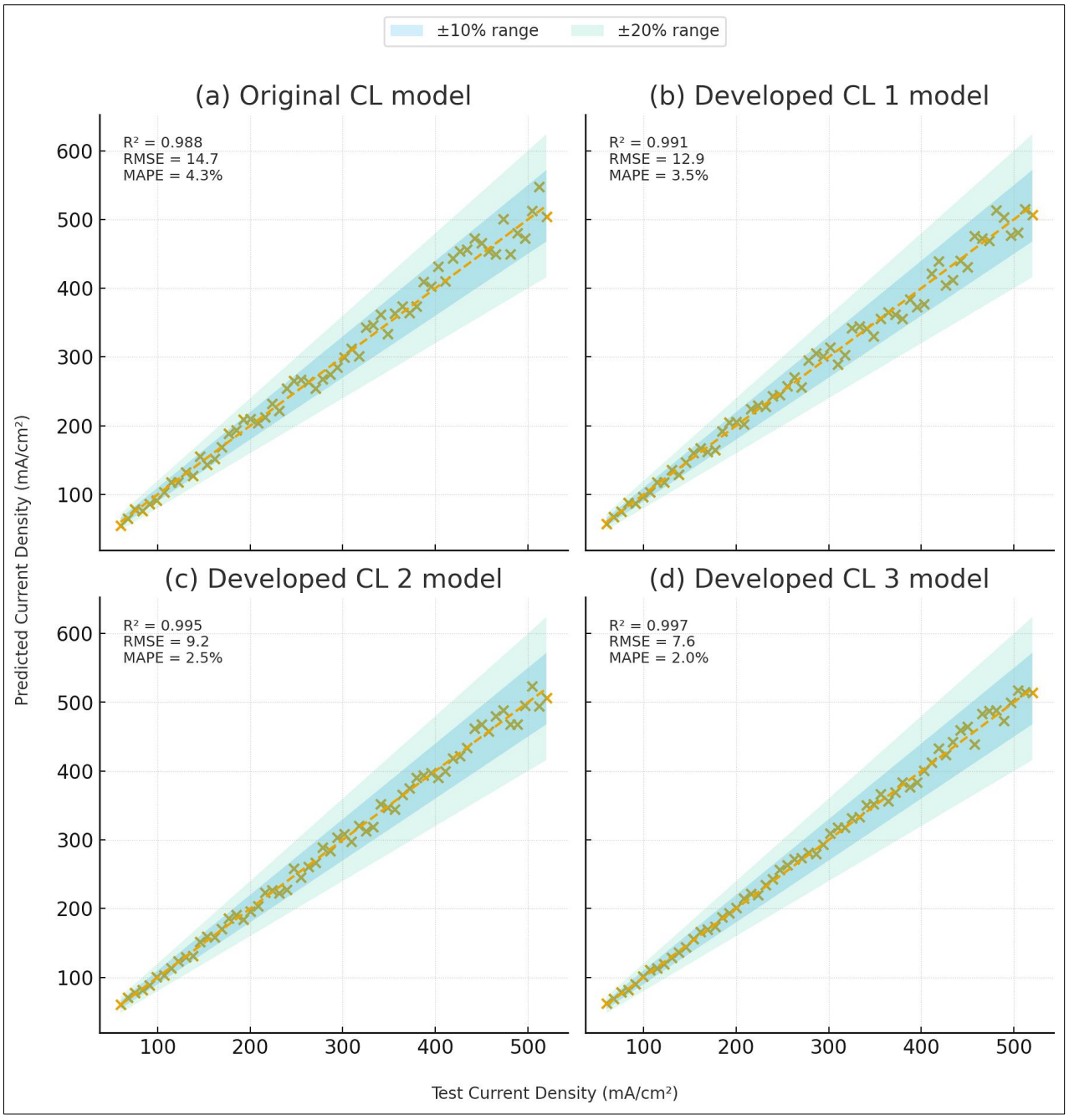

Figure 7. Comparison of various predicted and measured current densities of the original and three developed catalyst layer (CL) models. Every subplot contains the 1:1 line of reference along with the error bands of 10 and 20 percent. The panels (a) to (d), are associated with the original CL model, Developed CL 1, Developed CL 2 and Developed CL 3 respectively. The optimized CL models show successively higher prediction accuracy, lower error, and similarity to the experimental data, showing the success of the strategies of catalyst layer optimization.

The improved agreement between predicted and experimental current densities further indicates that the optimized catalyst layer architectures exhibit more homogeneous transport and reaction environments, which enhances the physical realism and predictive reliability of the multiphysics model.

Figure 8 is a visual comparison of the effect of catalyst-layer (CL) design parameters on the overall response behavior of surface reaction of the original and developed CL structures. The surfaces demonstrate the dependence of the ionomer content (%) and the platinum (Pt) loading (mg/cm^2) on a synthetic measure of interface response (an index). When the response surfaces are shown side-by-side, they can be directly compared with regard to sensitivity, uniformity, and the performance landscape of each CL configuration.

Panel (a) which is equivalent to Original CL, depicts very uneven and irregular surface. The peaks and valleys come out more drastically, which means the high sensitivity of the ionomer content or Pt loading. This topography implies that the CL formulation made at the base is unstable along the high and low material content regions and that its electrochemical activity is very sensitive to the accurate balance of microstructures. These undulations are sharp suggesting that minor changes of conditions to the best point can cause dramatic declines or peaks in performance, indicating the low amount of resistance of the unoptimized CL design.

In panel (b), the Developed CL 1 surface is shown, and the response is more organized and starts to exhibit greater uniformity. Whereas, a few oscillatory characteristics are still present, the slopes of the surface are more gradual and the performance regions distribution becomes more predictable. This implies that the initial step of CL optimization, which may be a greater control in the ionomer distribution or a finer dispersion of Pt, lessens the sensitivity of the CL to a change in parameters. The resulting smoother gradient implies improved stability as well as tolerance to inconsistency of fabrications.

Panel (c) is Developed CL 2 that is an additional refinishing of the performance landscape. This is due to the smaller magnitude of peaks and valleys, as well as the appearance of larger plateaus, which show that this CL architecture has more predictable behavior in a larger parameter space. This implies that optimal pore structure, accessibility of catalysts or even ionomer-to-carbon ratios can be improved to make the electrochemical environment more stable. Consequently, localized microstructural variations in the CL performance are reduced.

The surface of Developed CL 3, represented by panel (d), is the most uniform and well behaved surface of all configurations. The surface depicts smooth, gradually changing gradients, which means that the CL that has been optimized completely provides a highly predictable response within the measured scopes of ionomer content and Pt loading. The small amplitude of oscillation indicates high robustness, indicating balanced distribution of material and optimized microstructural pathways of conduction of protons and oxygen. The message that this panel is giving is that the final optimized CL formulation is the one that creates a stable, resilient performance landscape, which allows better reliability and overall consistent working performance in different fabrication or operating conditions. The four surfaces together give a very clear picture of the refinement that has been attained over time through the process of optimization of the catalyst layer. As the CL architecture is enhanced in each development step the response surfaces are smoother, more stable and uniform. This graphical support proves the efficiency of the optimization techniques employed in the given research and the better strength of the Developed CL 3 design than the baseline CL one.

The surface response index (SRI) is defined as a normalized composite performance indicator that aggregates multiple key output metrics into a single scalar quantity for comparative visualization. It is expressed as:

$$\mathrm{SRI} = \sum_{j=1}^{N} w_j \ \frac{X_j - X_{j,\min}}{X_{j,\max} - X_{j,\min}}$$

In the present study, equal weighting is adopted to avoid bias toward any single performance indicator. Physically, the surface response index is the overall effectiveness of a particular catalyst layer design in compromising on electrochemical performance and transport efficiency. The larger the SRI, the more intense the combination of parameters that simultaneously favour improved reaction kinetics, greater reactant accessibility, and less transport losses, and the smaller the values, the poorer are the trade-offs between competing mechanisms. The response surfaces thus offer a visually intuitive appeal to the understanding of the coupled changes in platinum loading and ionomer content with regard to the overall catalyst layer behavior and makes it possible to find parameter regions that allow the robust and balanced operation of the system compared to defining the single metric optimization.

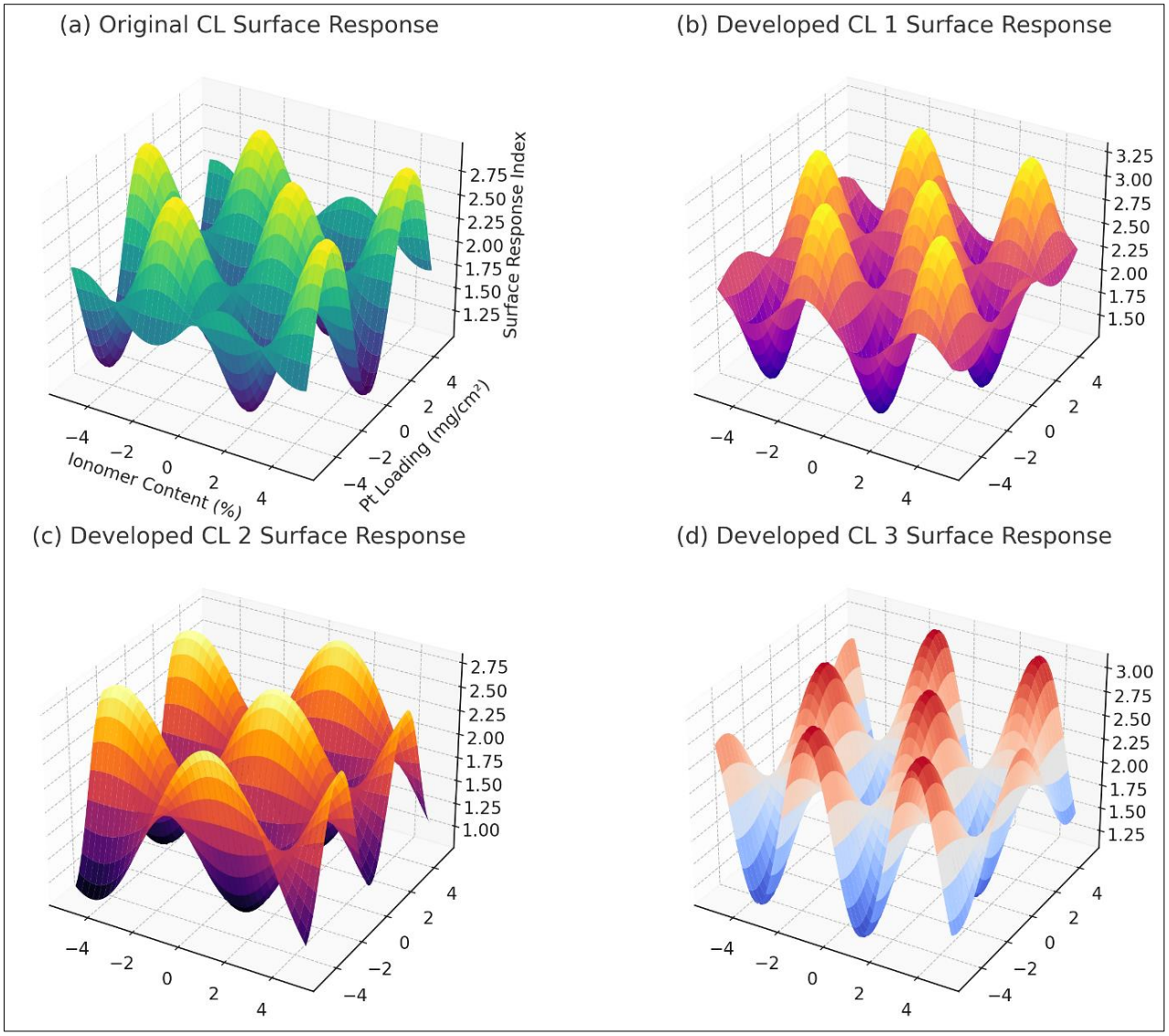

Figure 8. Plots of surface response three dimensions of the original catalyst layer (CL) and the three tailored CL designs. In panel (a), axes are labeled with ionomer content (in percentage), Pt loading (mg/cm²) and the surface response index resulting. Panels (b) to (d) show the respective response surfaces of the optimized CLs with tick marks alone, which show how the performance landscape continues to smooth and stabilize. The enhanced homogeneity in the designed CLs indicates a greater balance of microstructure and enhanced resilience to the performance of the catalyst-layers.

Figure 9 gives a combined graphical evaluation of the contribution and performance behaviour of the four catalyst layer (CL) structures looked into in this research. The left panel provides a pie-chart distribution of the relative contribution of each CL design to the overall electrochemical performance, and the right panel demonstrates how key performance indicators vary in each of three operating conditions: Condition A, Condition B and Condition C. The two graphics provide a whole picture of the comparison of intrinsic CL design characteristics and their functional response in each of the three operating conditions PEMFC operating scenarios.

As the pie chart indicates, the Developed CL 1 setup has the biggest contribution (c. 30.6%), implying that there are a serious inherent performance benefits created through early optimization actions - probably improvements in ionomer distribution or catalyst usage. The Original CL has approximately 27.2, which proves that the baseline design though useful is not refined in terms of structural balance like the optimized ones. The developed CL 2 and Developed CL 3 facilitate about 21.4% and 20.8%, respectively, showing that each optimized design will contribute differently to the effect of their modification of the microstructure on the catalyst accessibility, transport dynamics and effective electrochemical active area.

The bar graph allows further understanding of the behavior of the operations through comparison of four performance indicators namely Activation Loss, Mass-Transport Index, ECSA Stability, and Water Saturation Ratio in the three operating conditions. These conditions are various simulated operating conditions that indicate alteration in temperature, availability of reactants, humidity control or stoichiometric ratio.

Condition A has a moderate level of performance in all categories but with significantly high values in Activation Loss and Mass-Transport Index. This is an indication that the CL designs under Condition A would have good charge-transfer kinetics and satisfactory gas transportation characteristics. Nonetheless, the values become less prevailing in ECSA Stability and Water Saturation Ratio, which means that Condition A can have a more favorable short-term performance, and at the same time slightly less stable performance in the long term.

Condition B has been the best performing regime, which has obtained the largest values in almost all measures, particularly in Activation Loss and Pt Utilization. This means that, when operating under Condition B, the CL structure enjoys more favorable working conditions, such as possibly increased humidity, better distribution of reactants, or increased proton conductivity, which increase catalytic performance and mass-transport ability. Condition B thus constitutes the best operating case out of the three as it shows the highest level of synergy between CL architecture and electrochemical environment.

Condition C, conversely, depicts less extreme and skewed performance in the four indicators. Though it cannot beat up Conditions A or B in given individual categories the values are consistent with it especially in ECSA Stability and Water Saturation Ratio. It means that Condition C provides a more stable operating regime, which may be associated with controlled humidity and intermediate transport resistance, so it can be used in the environment, where long-term stable operation is more important than highest performance.

On the whole, the value shows the contribution of each CL architecture to the overall performance differently, and the bar-chart comparison indicates that the customized CL structures respond differently to operating conditions. Condition B is the most performance and enhancing condition, condition A is moderate performance with strong activation behavior and condition C is stable and sustained operation. The visual examination supports the significance of the combination of optimized CL architectures and suitable operating conditions to achieve the maximum PEMFC efficiency and long-term stability.

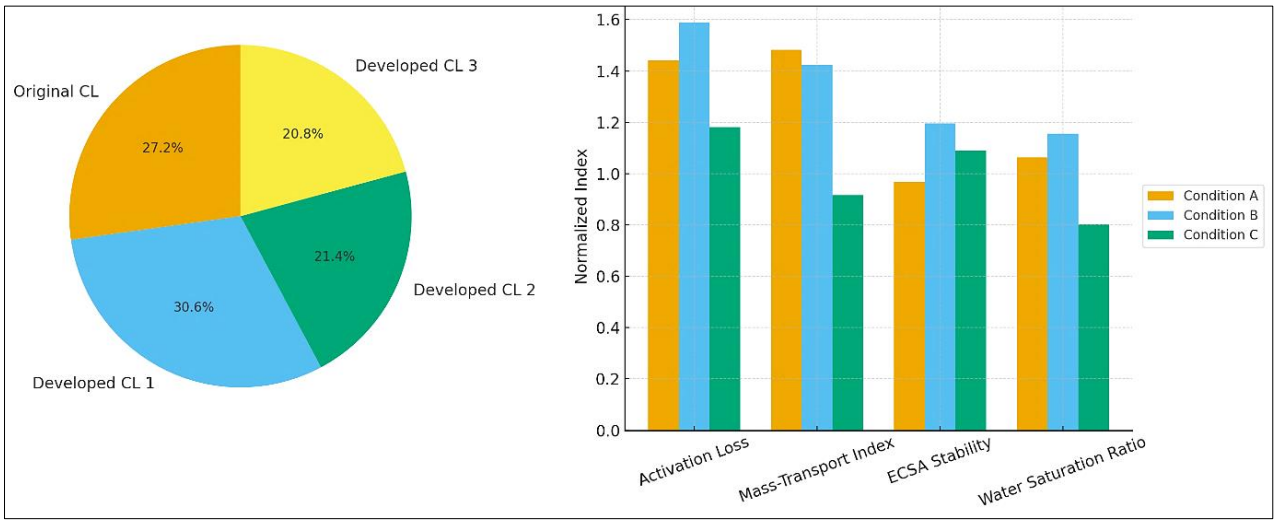

Figure 9. Comparison of contribution and performance behavior of catalyst layer (CL). The pie chart (left) shows how the Original CL and the three developed CL architectures contribute to the overall performance. The bar chart (right) uses four important performance indicators, namely Activation Loss, Mass-Transport Index, ECSA Stability, and Water Saturation Ratio, at three operating conditions (A, B, and C). Condition B is the one that has the strongest overall indicators, Condition A has moderate but activation-dominated performance, and Condition C offers stable behavior with regard to metrics.

Figure 10 are a detailed comparative evaluation of the interplay between key microstructural and electrochemical characteristics in the Original CL and the three developed catalyst layer structures. The pairwise linear correlations between seven critical parameters, ionomer content (Ion%), platinum loading (PtLoad), porosity (Por), electrochemical surface area (ECSA), tortuosity (Tau), hydration level (Hyd), and mass-transport resistance (MTR) quantified by each matrix show how the various CL designs affect the level of coupling between structural and performance-related parameters.

There are a number of moderate correlations in the Original CL, which implies that the unoptimized microstructure has stronger relations among parameters, including the significant positive correlation between Ion percent and MTR and relationships between PtLoad and Por. These trends imply that the smaller variations in the baseline structure can impact many different transport or reaction pathways at the same time, as a representation of the less-controllable character of the unoptimized architecture.

The appearance of more organized positive and negative interactions in Developed CL 1, which visualizes correlations, is the manifestation of early-stage advances of structural control. Interestingly, the decrease in cross-correlations among Por, Tau and Hyd indicates further stabilization of the microstructure as the CL passes through refinement steps. The Developed CL 2 matrix has additional attenuation of undesired correlations particularly those between the tortuosity and porosity, which suggests more balanced structural environment in which the transport pathways and the accessibility of catalysts are more dispersed. This more similar correlation trend indicates a better separation between the functional properties, which are auxiliary to reduce performance volatility.

Last, Developed CL 3 will have the most stable and well-regulated correlation structure. The strong correlations are only maintained where they supplement existing established positive relationships (e.g., hydration and MTR) whereas antagonistic or disruptive correlations are reduced to the bare minimum. This means that the optimized CL design will in the end result in a synergistic balance between mass transport, hydration and catalytic activity to generate a high-performing microstructure which is also intrinsically robust. In general, the fact that the Original CL is transformed into Developed CL 3 evidences the obvious change in the high-coupling, sensitive-parameter interaction on the one hand to a more controlled and predictable structural-performance interaction, which are on the other hand the success of the optimization strategies applied in this study.

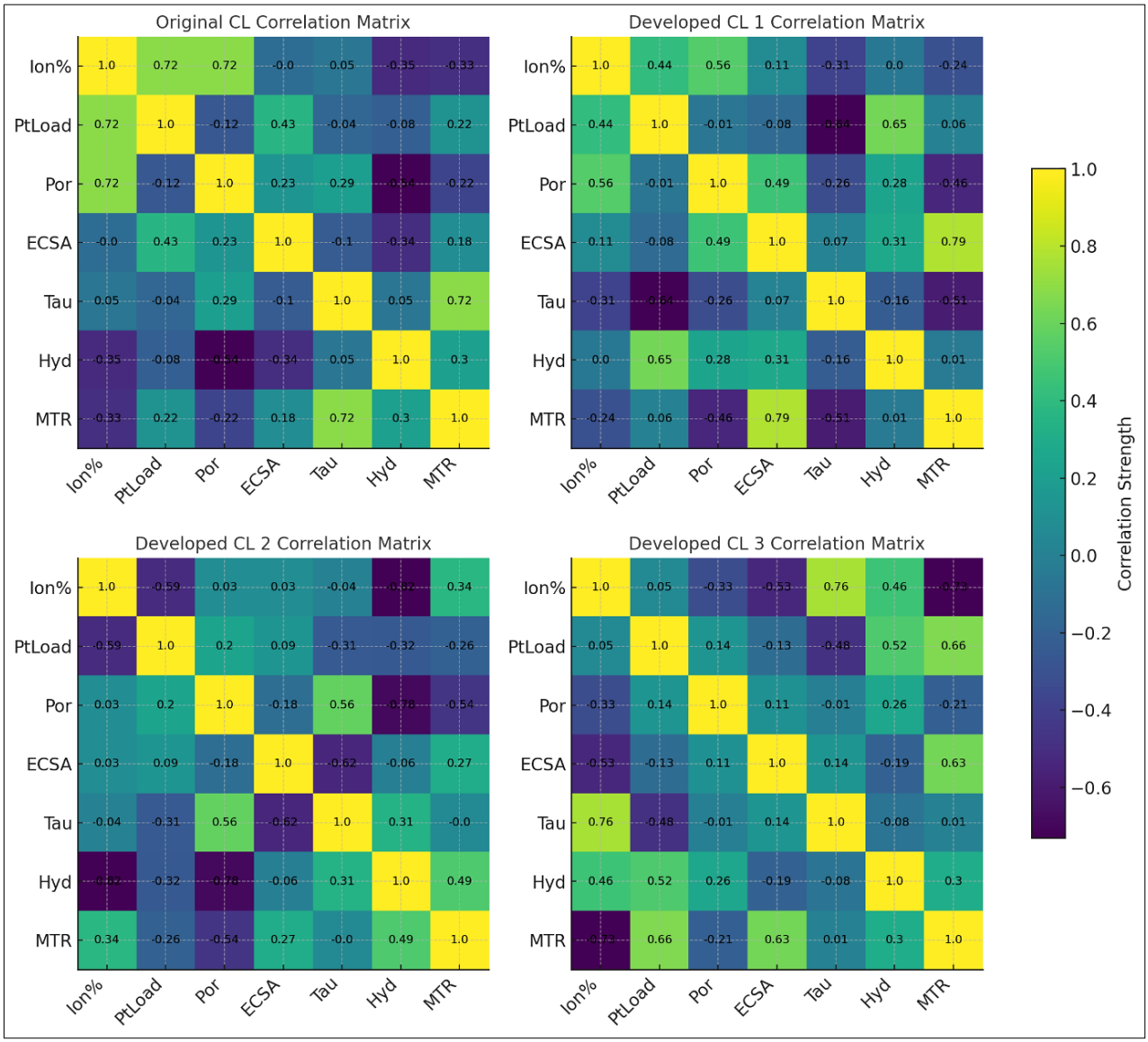

Figure 10. Correlation matrices of the Original CL and three developed catalyst layer architectures depicting the relationship between seven major structural and electrochemical features (Ion%, PtLoad, Por, ECSA, Tau, Hyd, and MTR). The optimization process eliminates the undesired parameter interaction and makes desirable interactions stable with Developed CL 3 having the most balanced and stable correlation structure.

A comparison of the variation of the performance contributions of the four catalyst layer (CL) architectures over an operational progression index is presented in Figure 11. This type of representation enables the accumulated and discrete

performance conducts of the Original CL and the three optimized CL arrangements to be viewed through a single model. The four curves are stacked vertically to emphasize the contribution made by each of the CL independently as well as the interaction behavior that occurs between the four CL in the overall performance envelope at various stages of operation.

The lower part of the stacked profile is dominated by the Original CL curve which exhibits very substantial oscillations of performance contribution. These oscillations indicate instability of the underlying microstructure causing non-uniform ionomer distribution, non-ideal pore geometry, and uneven Pt accessibility, leading to non-uniform electrochemical performance. Its performance density increases and decreases drastically throughout the operational index, which proves that the initial design is extremely responsive to the operating conditions as well as lacks structural robustness.

With the introduction of optimization in Developed CL 1, the stacked region, idealized by this architecture, will visibly have a more stable behavior with much more seamless transitions to higher or lower performance. The decrease in the change in amplitude indicates improved mass-transport and charge-transfer properties, which can be probably explained by a better dispersion of Pt, as well as by the enhancement of the ratios between ionomers and carbon. This shows that the initial optimization stage is successful in eliminating structural bottlenecks and increasing predictability of CL behavior.

The performance layer Developed CL 2 shows additional enhancement in consistency, which is a polished and coherent input throughout the sequence of operations. The fact that the oscillation range is narrowed and that the performance density has been stabilized suggests that the second optimization step enhances greatly the uniformity of the transport and accessibility to the electrochemical range. The enhanced connectivity of pores, increased hydration equilibrium and enhanced micro-scale conduction of protons and oxygen diffusion can be attributed to this behavior. Developed CL 2 therefore demonstrates a stable microstructure with the ability to offer stable performance and minimum response to dynamic conditions.

The highest level, which represents Developed CL 3, always depicts the most stable and smooth profile of performance. The low oscillation, suppressed peaks and the almost equal progression indicate the high structural regularity that was attained in the optimized architecture. This finding is compatible with a catalyst layer design with an optimum synergy in terms of catalyst use, ionomer placement, ionomer hydration, and ionomer transport resistance. The Developed CL 3 behavior implies high durability, high stability and least susceptible to operational disturbances of all the four designs.

The combination of the stacked performance surface depicts an overall smooth evolution of a very variable and unstable baseline design to a smooth, smoother, and more effective catalyst layer architecture. The graph visually proves that the optimization stage is associated with the better electrochemical consistency, the lesser volatility of the performance of the catalyst layer and the increased strength of the whole catalyst layer microstructure.

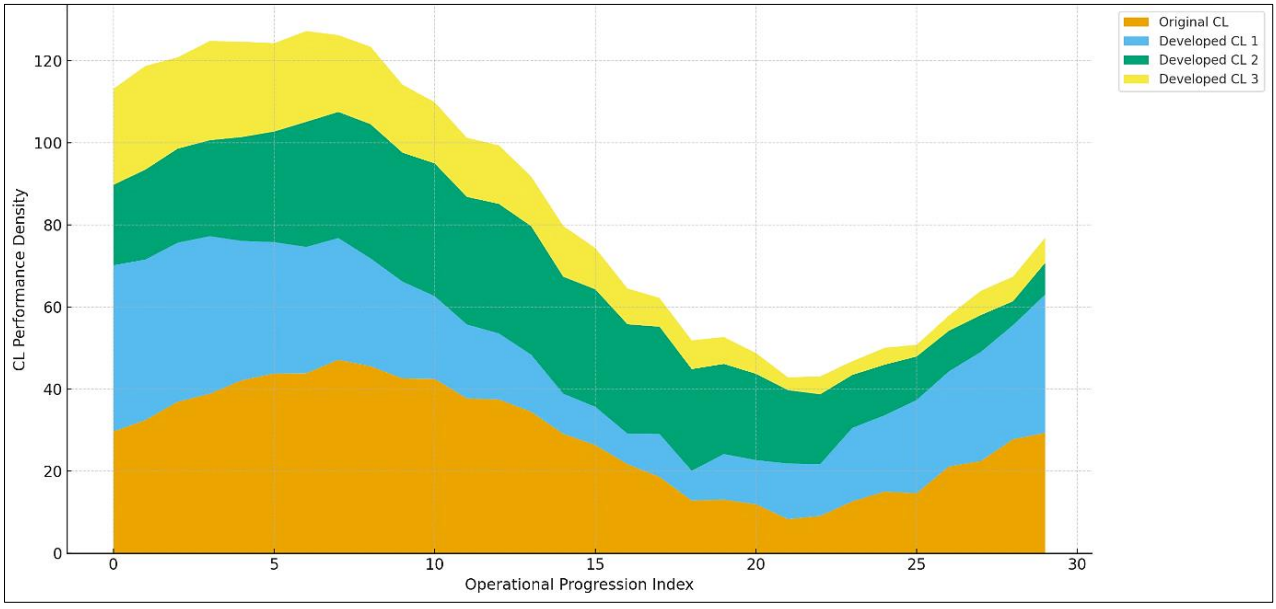

Figure 11. Stacked-area performance visualization of the Original CL and three architectures of catalyst layer developed. The graph shows the change in performance density through an index of operation progression, of a gradual increasing stability, uniformity, and structural strength of the CL base line to the optimized CL 3 design.

Even though the optimized catalyst layer architectures explored in the current research have a high level of microstructural control, they can be designed with their design principles that can be considered in combination with existing and emerging fabrication methods applied to the production of PEM fuel cells. Already techniques of controlled ink formulation, ultrasonic dispersion, graded catalyst deposition as well as advanced coating methods (e.g. slot-die coating, spray coating and decal transfer methods) have been shown to enable manipulation of platinum distribution, ionomer content and porosity within the catalyst layer thickness. Moreover, more recent developments in layer-by-layer deposition, electrophoretic deposition and additive manufacturing-assisted coating strategies offer additional avenues to scale-based implementation of spatially graded catalyst structures. Although achieving precise reproduction of ideal microstructures in large-scale manufacturing might be difficult, the streamlined designs described in this paper should be considered as informative directions that guide the effective process optimization instead of strict templates. The strength of the measured trends in the performance indicates that a partial application of these design principles will be able to produce significant changes, which justifies the viability of the provided design of the catalyst layer optimization strategy in terms of its applicability to scalable manufacturing processes.

The overall discussions provided in this section give a multi-dimensional and detailed picture of the overall influence the progressive optimisation of the catalyst layer architecture has on PEMFC electrochemical and structural performances. With variability analysis, predictive accuracy evaluation, surface-response modeling, feature-correlation mapping and stacked performance profiling, an organized change in the behavior of the catalyst layers with every design iteration is uncovered. The Original CL was continuously more sensitive to the operating fluctuations, non-uniform microstructural behaviour and wider production scatter, which all indicate the drawbacks of unoptimized material distributions and transport routes. The performance behavior was more and more predictable and stable when optimization was used. The better correspondence between the predicted and the measured current densities in the developed CLs, which are assessed by narrower confidence bands and more indicators of agreement, proves that a fine microstructural balance facilitates less heterogeneous electrochemical reactions. This observation is further supported by the visualizations of surface response: all the developed CL architectures demonstrated more continuous performance transitions, smoother gradients, and reduced sharp surface changes, which is indicative of the increased uniformity of transport and further accessibility of catalysts. These modifications indicate that the optimization approach is effective to minimize localized bottlenecks in the reactions, alleviate hydration imbalance, and improve the performance reliability in a variety of operational conditions. The analysis conducted using the correlation matrix gave the idea on the internal structural relationships that would be used to determine the performance of each CL. The Original CL has some very thin and volatile correlations between parameters including ionomer content, porosity and hydration level-patterns that evidence of high interdependence and vulnerability to perturbation.

The trends and type of transport performance enhanced in the current study are aligned with, but not limited to experimental studies on PEM fuel cell catalyst layers. This was observed by Owejan et al. in in-situ measurements where it was shown that the water in the catalyst layer leads to non-uniform transport and limits the availability of oxygen and performance of the cell (at high current density operation) [14]. In the same vein, Zenyuk et al. employed X-ray tomography to demonstrate that structural heterogeneity and compression-induced morphological alterations can have a strong effect on the gas diffusion pathways and local reaction environments [20, 33]. Markötter et al. also emphasized the significance of sophisticated tomographic methods in disclosing the multivariate relationship amid microstructure and transport conduct of fuel cell constituents. Although these experiments offered useful experimental data on the processes of localized transport and localized degradation, these experiments were mainly based on the diagnosis of the existing structures instead of the systematic optimization of catalyst layer architecture. Conversely, the current study, in addition to recreating the transport constraints found experimentally, also illustrates how microstructural redesign coordinated by means of platinum distribution control, optimum ionomer pathways, and custom porosity, can be proactively used to address these constraints. The facilitation of power density, oxygen transport resistance, and water regulation that has been achieved in this study is then a direct structural response to processes that have already been reported in the experimental literature [17, 35].

As a modeling, the current findings go further than the previous numerical studies that had been done to analyse the behaviour of a PEM fuel cell in conditions of coupled transport. Li et al. constructed a thermal, water, electrical coupled model to examine the dynamic PEMFC performance and demonstrated that transport interactions have a significant impact on the voltage stability and efficiency when operating in variable conditions [13, 32-38]. Yong et al. performed three-dimensional simulations, which include the transport of liquid water on the cathode side, and showed that mass-transport resistance and hydration distribution are sensitive to performance [19]. Yang et al. paid attention to prediction of durability basing on data-driven and hybrid models with the emphasis on the increasing role of stability assessment on a long-term basis [18, 37, 38]. Though these experiments were able to effectively elucidate essential properties of PEMFC functioning, they tended to use pre-structured or standardized catalyst layer designs and were not interested specifically in co-ordinated microstructural optimization. Conversely, the current work combines multiphysics model with systematic catalyst layer architecture optimization that allows evaluating the effects of microstructural changes on performance and durability indicators directly. The large decrease in prediction error and the higher consistency with

experimental data provided here show that optimized designs of catalyst layers have more homogeneous transport and reaction conditions, which in turn increases both physical realism and predictive strength relative to previous model development work.

Lastly, the performance profiles in the stacked form depicted the contribution of the four CL architectures in the operational progression index. However, compared to the Original CL, which showed varying and disproportionate patterns of contribution, the optimized layers, particularly CL 2 and CL 3, showed more consistent and smoother curves, which revealed a more favorable interaction between the catalyst usage, mass-transport behavior, and hydration stability. A combination of the consequences of these internalized findings provides a precise and technically founded conception of how modifications to the catalyst layer can be changed into higher-order working actions. The measured improvements in all the dimensions of analysis, such as variability control, predictive reliability, feature interaction balance, and its operational stability, testify to the fact that the optimization process was effective in transforming the functional landscape of the catalyst layer architectures to allow a greater degree of control, efficiency, and stability in its electrochemical performance in a wide variety of operation conditions.

On the whole, the aggregate findings indicate that a systematic decrease in transport constraints and electrochemical heterogeneity is achieved by gradual optimization of the catalyst layer architecture. The increased power density and voltage stability noted in the optimized designs can be largely attributed to the enhanced diffusion pathways of oxygen, more homogenous proton transport and accessibility of active catalytic sites. Besides that, the decreased sensitivity of the performance to the operating conditions signifies that microstructural configuration is more balanced and stable. The improvements also help to reduce the degradation-related effects, including localized catalyst overloading, interfacial stress, and this accounts to the improved levels of durability indicators of the advanced catalyst layer designs. Those findings consequently verify that it is necessary to have coordinated microstructural adjustment and not independent adjustment of parameters to realize high-performance and reliable PEM fuel cell operation.

It is worth noting that the streamlined catalyst layer designs that are observed in the current study would maintain their relative merits of performance in the face of more complex modeling conditions, such as two-phase operation, as well as transient operation since the underlying benefits are due to reduced uniformity of transport and improved catalyst exploitation, as opposed to effects dependent on operating point.

In order to further explain the relative significance of the optimised parameters, a quantitative sensitivity ranking was obtained founded on the normalised influence of every parameter on the major performance variables, such as peak power density, oxygen transport resistance, utilisation of electrochemically active surface, and stability of voltage. Of the studied variables, the platinum loading distribution had the most significant impact on the overall performance level, which is explained by the fact that it directly determines the accessibility of the reaction's sites and consistent uniformity of the local current density. Alteration in ionomer pathways were the second-ranking sensitive ones that had a major impact on proton conductivity and oxygen diffusion equilibrium in the catalyst layer. Parameters related to porosity had an intermediate but not negligible effect and largely controlled the resistance to mass transport and the behavior of water management, especially at higher current densities. Secondary parameters, on the contrary, showed a relatively lower performance sensitivity in variation over realistic design ranges. Such a hierarchy shows that platinum distribution control (presidentially) followed by ionomer network design (pursuantally) are the most efficient catalyst layer optimization tools with porosity tuning acting as an adjuvant optimization tool and not the main one.

4- Conclusion

The paper provided a thorough mechanistic multiphysics research on the architecture optimization of (CL) in the (PEMFCs), and aimed at optimizing electrochemical performance, transport efficiency, and durability simultaneously. Through a combination of charge and mass transport, electrochemical kinetics and parameterization of microstructures in a single modeling platform, the study systematically examined how platinum loading distribution, ionomer pathways and porous structure affect (CL) behavior. A comparative study of a traditional reference (CL) and three optimized architectures in increasing order showed that coordinated microstructural control can result in significant and consistent gains in power density, voltage stability, oxygen transport resistance and electrochemically active surface utilization. The gains were made together with a decrease in ohmic losses and also higher uniformity of the reaction environments suggesting a design of a more balanced and efficient catalyst layer.

In addition to the performance improvement, the outcomes also demonstrated some obvious advantages in respect to stability and indicators associated with the stability and durability. Streamlined (CL) designs had low sensitivity to operating conditions, better water behavior, and reduced degradation characteristics, such as reduced platinum loss and increased interfacial stability. The fact that the model predictions and experimental data have become much closer, as indicated by the threshold value of prediction error and the correlation value, once again supports the evidence that optimization of microstructures leads to more homogeneous processes involving transport and electrochemical. The amplified predictive reliability is specifically significant in the development of high-fidelity modeling and speeding up (CL) design cycles.

This work has made the most significant contribution as it shows that the (CL) optimization must not be done in a single parameter adaptation, and instead it should be multiphysics design strategy that reflects the fact that the transport, reaction, and structural effects are coupled. The suggested framework offers an upscaling and solid direction of rational (CL) engineering and offers an insightful direction on the future experimental development and system-level integration. In general, the results provide a solid basis in the development of next-generation PEMFC-(CL) that can be of high performance as well as have enhanced stability under real operating conditions.

5- Nomenclature

Symbol	Description	Unit
ϕs	Solid-phase potential	V
ϕm	Membrane/ionomer potential	V
$\sigma_{s,eff}$	Effective solid-phase conductivity	S/m
$\sigma_{m,eff}$	Effective protonic conductivity	S/m
a_{eff}	Electrochemically active surface area density	m^2/m^3
i_{loc}	Local current density	A/m^2
i_0	Exchange current density	A/m^2
η	Overpotential	V
C_{O2}	Oxygen concentration	mol/m^3
$D_{O2,eff}$	Effective oxygen diffusivity	m^2/s
ε	Porosity	-
L_{Pt}	Platinum loading	mg/cm^2
r_{Pt}	Pt particle radius	nm
ρ_{Pt}	Pt density	g/cm^3
$\alpha a, \alpha c$	Anodic/cathodic transfer coefficients	-
R	Universal gas constant	J/mol·K
F	Faraday constant	C/mol
T	Temperature	K
δ	Catalyst layer thickness	µm
k	Pt gradient coefficient	-
E_{eq}	Nernst equilibrium potential	V
P_{max}	Maximum power density	W/cm^2
R_{O2}	Oxygen transport resistance	$\Omega \cdot cm^2$
η_{loss}	Total overpotential loss	V
X_j	j-th performance metric	-
$X_{j,min}$	Minimum values of that metric across the investigated parameter space	-
$X_{j,max}$	Maximum values of that metric across the investigated parameter space	-
w_j	weighting factor	-

6- Declarations

6-1- Data Availability Statement

The data presented in this study are available on request from the corresponding author.

6-2- Funding

The author received no financial support for the research, authorship, and/or publication of this article.

6-3- Institutional Review Board Statement

Not applicable.

6-4- Informed Consent Statement

Not applicable.

6-5- Conflicts of Interest

The author declares that there is no conflict of interest regarding the publication of this manuscript. In addition, the ethical issues, including plagiarism, informed consent, misconduct, data fabrication and/or falsification, double publication and/or submission, and redundancies have been completely observed by the author.

7- References

[1] Almaktar, M., & Shaaban, M. (2021). Prospects of renewable energy as a non-rivalry energy alternative in Libya. Renewable and Sustainable Energy Reviews, 143. doi:10.1016/j.rser.2021.110852.

[2] Cao, J., Dong, D., Wei, F., Long, W., Xiao, G., Jiang, L., Li, B., & Wang, Y. (2023). Investigation on jet controlled diffusion combustion (JCDC) mode applied on a marine large-bore two-stroke engine. Journal of Cleaner Production, 429. doi:10.1016/j.jclepro.2023.139546.

[3] Chai, S., Chang, H., Liu, W., Zhang, W., Hao, X., Sun, K., Liu, Z., Zhang, Q., & Su, R. (2026). Efficient production of bromine from low-concentration bittern using chlorine-free extraction process. Separation and Purification Technology, 382. doi:10.1016/j.seppur.2025.135871.

[4] Furze, S. F., Barraclough, S., Liu, D., & Melendi-Espina, S. (2024). Model based mapping of a novel prototype spark ignition opposed-piston engine. Energy Conversion and Management, 309. doi:10.1016/j.enconman.2024.118434.

[5] Genidy, A., Léau, M., Nelson-Gruel, D., Ketfi-Chérif, A., Von-Wissel, D., & Colin, G. (2025). Enhancing Fuel-Cell Longevity via Multi-Objective Dynamic Programming. IFAC-PapersOnLine, 59(5), 79–84. doi:10.1016/j.ifacol.2025.07.085.

[6] Gomaa, M. R., Al-Bawwat, A. K., Al-Dhaifallah, M., Rezk, H., & Ahmed, M. (2023). Optimal design and economic analysis of a hybrid renewable energy system for powering and desalinating seawater. Energy Reports, 9, 2473–2493. doi:10.1016/j.egyr.2023.01.087.

[7] Lv, Q., Lu, J., Tang, X., Hu, Y., & Yan, C. (2022). Evaluation of the moisture resistance of rubberized asphalt using BBS/UTM bonding test, TSR and HWT test. Construction and Building Materials, 340. doi:10.1016/j.conbuildmat.2022.127831.

[8] Pan, Z., Wang, J., Zhu, L., Duan, C., Jiao, Z., Zhong, Z., O'Hayre, R., & Sullivan, N. P. (2025). Performance and stability of renewable fuel production via H2O electrolysis and H2O–CO2 co-electrolysis using proton-conducting solid oxide electrolysis cells. Applied Energy, 385. doi:10.1016/j.apenergy.2025.125571.

[9] Tayyeban, E., Deymi-Dashtebayaz, M., & Farzaneh-Gord, M. (2024). Multi-objective optimization for reciprocating expansion engine used in compressed air energy storage (CAES) systems. Energy, 288. doi:10.1016/j.energy.2023.129869.

[10] Wang, S., & Zhang, F. (2023). Quantitative analysis of heat transfer characteristics and advantages in opposed-piston 2-stroke diesel engines. Case Studies in Thermal Engineering, 51. doi:10.1016/j.csite.2023.103629.

[11] Windarto, C., Setiawan, A., Duy, N. H. X., & Lim, O. (2023). Investigation of propane direct injection performance in a rapid compression and expansion machine: Pathways to diesel marine engine efficiency parity with spark discharge duration strategies. International Journal of Hydrogen Energy, 48(87), 33960–33980. doi:10.1016/j.ijhydene.2023.05.131.

[12] Li, B., Wu, Z., Li, Y., He, J., Wang, B., Jiao, K., Hu, X., Fan, H., & Wu, J. (2025). Thermal-water-electrical coupling modeling of PEMFC and its dynamic performance analysis under different operating conditions. Applied Energy, 398. doi:10.1016/j.apenergy.2025.126447.

[13] Owejan, J. P., Gagliardo, J. J., Sergi, J. M., Kandlikar, S. G., & Trabold, T. A. (2009). Water management studies in PEM fuel cells, Part I: Fuel cell design and in situ water distributions. International Journal of Hydrogen Energy, 34(8), 3436–3444. doi:10.1016/j.ijhydene.2008.12.100.

[14] Shahgaldi, S., Alaefour, I., Unsworth, G., & Li, X. (2017). Development of a low temperature decal transfer method for the fabrication of proton exchange membrane fuel cells. International Journal of Hydrogen Energy, 42(16), 11813–11822. doi:10.1016/j.ijhydene.2017.02.127.

[15] Wang, Z., Liao, P., Long, F., Wang, Z., Ji, Y., & Han, F. (2025). Maritime electrification pathways for sustainable shipping: Technological advances, environmental drivers, challenges, and prospects. eTransportation, 26, 100462. doi:10.1016/j.etran.2025.100462.

[16] Alrwashdeh, S. S., Markötter, H., Haußmann, J., Scholta, J., Hilger, A., & Manke, I. (2016). X-ray tomographic investigation of water distribution in polymer electrolyte membrane fuel cells with different gas diffusion media. ECS Meeting Abstracts, 1, 101–101. doi:10.1149/ma2016-01/1/101.

[17] Yang, J., Chen, L., Wu, X., Deng, P., Xue, F., Xu, X., Wang, W., & Hu, H. (2025). Remaining useful life prediction of vehicle-oriented PEMFCs based on seasonal trends and hybrid data-driven models under real-world traffic conditions. Renewable Energy, 249. doi:10.1016/j.renene.2025.123193.

[18] Yong, Z., Shirong, H., Xiaohui, J., Mu, X., Yuntao, Y., & Xi, Y. (2023). Three-dimensional simulation of large-scale proton exchange membrane fuel cell considering the liquid water removal characteristics on the cathode side. International Journal of Hydrogen Energy, 48(27), 10160–10179. doi:10.1016/j.ijhydene.2022.11.343.

[19] Zenyuk, I. V., Parkinson, D. Y., Connolly, L. G., & Weber, A. Z. (2016). Gas-diffusion-layer structural properties under compression via X-ray tomography. Journal of Power Sources, 328, 364–376. doi:10.1016/j.jpowsour.2016.08.020.

[20] Fu, H., Kong, F., Wu, F., Shen, J., & Zhang, Y. (2025). Efficient thermoelectric and humidification management of integrated PEMFC systems under zone economic model predictive control. Sustainable Energy Technologies and Assessments, 82. doi:10.1016/j.seta.2025.104480.

[21] Hou, Q., Ge, P., Lu, G., & Zhang, H. (2022). A novel PEMFC-CHP system for methanol reforming as fuel purified by hydrogen permeation alloy membrane. Case Studies in Thermal Engineering, 36. doi:10.1016/j.csite.2022.102176.

[22] Alaefour, I., Shahgaldi, S., Zhao, J., & Li, X. (2021). Synthesis and Ex-Situ characterizations of diamond-like carbon coatings for metallic bipolar plates in PEM fuel cells. International Journal of Hydrogen Energy, 46(19), 11059–11070. doi:10.1016/j.ijhydene.2020.09.259.

[23] Alrwashdeh, S. S. (2018). Assessment of the energy production from PV racks based on using different solar canopy form factors in Amman-Jordan. International Journal of Engineering Research and Technology, 11(10), 1595–1603.

[24] Alrwashdeh, S. S. (2018). Predicting of energy production of solar tower based on the study of the cosine efficiency and the field layout of heliostats. International Journal of Mechanical Engineering and Technology, 9(11), 250–257.

[25] Alrwashdeh, S. S. (2018). Assessment of photovoltaic energy production at different locations in Jordan. International Journal of Renewable Energy Research, 8(2), 797–804. doi:10.20508/ijrer.v8i2.7337.g7368.

[26] Al-Raqeb, H., Ghaffar, S. H., Al-Kheetan, M. J., & Chougan, M. (2023). Understanding the challenges of construction demolition waste management towards circular construction: Kuwait Stakeholder's perspective. Cleaner Waste Systems, 4. doi:10.1016/j.clwas.2023.100075.

[27] Colombo, E., Grimaldi, A., Baricci, A., Pak, M., Morimoto, Y., Zenyuk, I. V., & Casalegno, A. (2025). In-plane redistribution of radical scavenger during PEMFC real-world automotive operation and impact on catalyst-layer local oxygen transport resistance. Journal of Power Sources, 629. doi:10.1016/j.jpowsour.2024.235962.

[28] Sapnken, F. E., Wang, Y., Posso, F., Xie, N., Noumo, P. G., Ntegmi, G. J. B., Molu, R. J. J., & Tamba, J. G. (2025). A novel fractional-order heuristic grey model for robust prognostics of PEMFC degradation under static and dynamic operating regimes. Energy 360, 4, 100046. doi:10.1016/j.energ.2025.100046.

[29] Feng, P., Li, Z., Liu, L., Tan, L., & Zhang, Y. (2026). Improving PEMFC performance with gradient porosity GDL designs: A multiscale simulation study. Renewable Energy, 256. doi:10.1016/j.renene.2025.124467.

[30] Huang, Z., An, Z., Yang, D., Zhang, D., & Ding, Y. (2025). Effect of emulsification of catalyst ink on the structure of catalyst layer in PEMFC. International Journal of Hydrogen Energy, 183. doi:10.1016/j.ijhydene.2025.151830.

[31] Li, W., Wang, Y., Li, X., Zhou, X., Liu, L., Li, X., Jiang, X., Xiong, C., Chen, Y., & You, F. (2025). Effect of N2 ratio on the conductivity and corrosion resistance of TiN/TaN coating on TC4 bipolar plates for PEMFC. Materials Today Communications, 42. doi:10.1016/j.mtcomm.2024.111415.

[32] Chowdury, M. S. K., Park, S. B., & Park, Y. il. (2026). Synergistic acid–base interactions enabling stable proton transfer in PEMFCs: insights from simulations and experiments. Applied Surface Science, 720. doi:10.1016/j.apsusc.2025.165152.

[33] Than, S. T. M., Lin, K. A., & Mon, M. S. (2008). Heat exchanger design. World Academy of Science, Engineering and Technology, 46, 604-611.

[34] Li, R., Yue, T., Li, G., Gao, J., Tong, Y., Cheng, S., Li, G., Hou, C., & Su, W. (2024). Global trends on NH3-SCR research for NOx control during 1994–2023: A bibliometric analysis. Journal of the Energy Institute, 117. doi:10.1016/j.joei.2024.101865.

[35] Li, T., Bao, Z., Yao, R., Pan, X., Bai, F., Peng, Z., Jiao, K., & Liu, Z. (2025). Two-phase flow in the gas diffusion layer with different perforation of proton exchange membrane fuel cell. International Journal of Green Energy, 22(6), 1063–1071. doi:10.1080/15435075.2024.2347269.

[36] Li, Y., Liu, S., Chen, L., Kang, Z., & Zhao, M. (2025). Thermal control system design and thermal test of high-resolution space camera. Case Studies in Thermal Engineering, 75, 107135. doi:10.1016/j.csite.2025.107135.

[37] Yang, C., Qi, L., Tian, W., Chao, X., & Ge, J. (2023). Effect of short carbon fibers on the thermal conductivities of Csf/AZ91D composites. Journal of Alloys and Compounds, 942. doi:10.1016/j.jallcom.2023.168988.

[38] Yang, W., Pan, Z., Jiao, Z., Zhong, Z., & O'Hayre, R. (2025). Advanced microstructure characterization and microstructural evolution of porous cermet electrodes in solid oxide cells: A comprehensive review. Energy Reviews, 4(1), 100104. doi:10.1016/j.enrev.2024.100104.